SPACECRAFT DEPARTMENT

MISSILE AND SPACE DIVISION

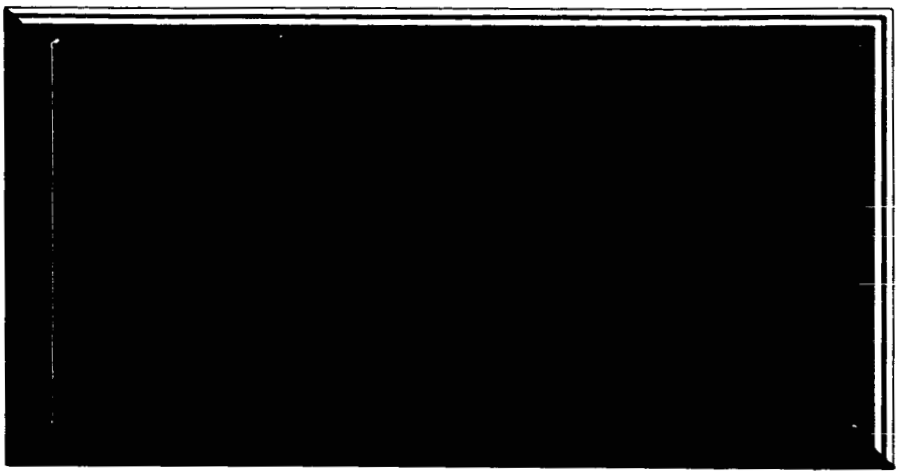

GPO PRICE $ _____

CFSTI PRICE(S) $ _____

Hard copy (HC) 3.00

Microfiche (MF) .50

ff 653 July 65

FACILITY FORM 602

N67 13198 (ACCESSION NUMBER)

54 (PAGES)

CR-80517 (NASA CR OR TMX OR AD NUMBER)

(THRU)

1 (CODE)

15 (CATEGORY)

GENERAL ELECTRIC

DIN 66SD4530
1 NOVEMBER 1966

DEVELOPMENT OF ENERGY DISSIPATING PLASTIC HONEYCOMB QUARTERLY PROGRESS REPORT NO. 5 AUGUST 1, THROUGH OCTOBER 31, 1966

CONTRACT NO. 951172

CALIFORNIA INSTITUTE OF TECHNOLOGY
(JET PROPULSION LABORATORY)
4800 OAK GROVE DRIVE
PASADENA, CALIFORNIA

This work was performed for the Jet Propulsion Laboratory, California Institute of Technology, sponsored by the National Aeronautics and Space Administration under Contract NAS7-100.

GENERAL ELECTRIC

SPACECRAFT DEPARTMENT

A Department of the Missile and Space Division
Valley Forge Space Technology Center
P.O. Box 8555 • Philadelphia 1, Penna.

TABLE OF CONTENTS

LIST OF ILLUSTRATIONS

LIST OF TABLES

SECTION 1
SUMMARY

Two major changes are being incorporated into this contract. These changes consist of the addition of (1) more elaborate tooling (to fabricate the dovetail specimens) and (2) an investigation to determine the effect on energy absorption of adding glass filler materials to the dip resin used in manufacturing honeycomb specimens.

Because of these major changes, the resulting contract completion date is now April 30, 1967. However, a target completion date of March 31, 1966, is being scheduled; every effort will be made to complete the program by this earlier date.

Manufacturing problems still exist in fabricating the handmade dovetail specimens. The procedures used to fabricate the material have been changed once again. When these new procedures are introduced into the manufacturing process, it is believed that all problems will be eliminated. Fabrication of the first specimen, using these new procedures, is scheduled during the first week of November 1966.

The design of all tooling required to fabricate the large dovetail specimens has been completed, and all long lead time items have been ordered. The fixture to be used for curving the dovetail specimens has been designed and is in the process of being procured.

Investigation has been initiated of the addition of filler material to the dip resin and has shown that it is feasible to modify the existing dip resin with either short fibers or flakes of glass. The next step in the program will be the fabrication of honeycomb specimens to be used for testing.

Static and high velocity tests have been conducted on the hexagonal cell. Static tests of the hexagonal cell, thinned dip improved bond, honeycomb have been conducted at temperatures of +200^{o}F and -100^{o}F. Performance is excellent at -100^{o}F and relatively poor at +200^{o}F. High velocity tests, performed thus far, have shown that the hexagonal cell material performance at high velocity is equal to, or greater than, the performance of those measured on static tests.

AUTHOR

SECTION 2

PROGRAM REVISION

2.1 DISCUSSION

Based on results of technological developments and findings during the performance of this contract thus far, General Electric and the customer agreed that a change in the scope of this contract would be benificial at this time. Two major changes were therefore incorporated into the contract and are as follows:

1. Replace the standard corrugated method of fabricating the dovetail design, with a newly developed method which uses special tooling for forming and assembling a dovetail design specimen;

2. Investigate the possible advantages of adding glass fibers or glass flakes to the dip resin used to fabricate plastic honeycomb material.

From the fabrication of dovetail specimens by the corrugated method, it was found that the crushing strength of the resulting material was very low. This low crushing strength is attributable to the low strength of the node line bond joints. Also, the cell configurations varied widely throughout the specimens. In the corrugated method of fabricating the material, it is necessary to use a node bond line adhesive which has different properties than the adhesive used in fabricating the optimum design hexagonal-shaped cell core material developed in this program. To use the optimum adhesive, it is necessary to exert pressure on the node bond line during the cure cycle of the adhesive. This effect is not possible in the fabrication of a dovetail design specimen by the corrugated method. A new fabrication method was, therefore, developed which enables pressure to be exerted on the node bond line during adhesive curing. The use of this method also produces a good-shaped cell configuration throughout the material. Use of the recommended tooling permits fabrication of special dovetail specimens at a unit cost, which is equal to, or lower than, the specimen cost of special hexagonal-shaped cell configurations.

During this program, it has been established that the resin, rather than the glass cloth, is the main contributor to the high energy absorbing properties of the optimum design plastic

honeycomb. Therefore, if the crushing strength of the resin is increased, the crushing strength of the core material should be increased. Filling of the resin used in fabricating the honeycomb material with glass fibers or flakes should increase the crushing strength of the resin and therefore the crushing strength of the honeycomb material. A program was therefore added that includes the required process investigation necessary to include this filler material in the dip resin and fabrication and testing of specimens fabricated in this manner.

The increase in scope of the existing program therefore results from special tooling requirements to fabricate the dovetail specimens and to conduct an investigation of using fillers in the resin required to fabricate plastic honeycomb.

2.2 SCHEDULE CHANGE

The new schedule, which permits the incorporation of these required changes, requires that the contract be completed no later than April 30, 1967. However, a target completion date of March 31, 1967, is desired by the customer, and every effort will be made to meet this date. In view of this shorter target date, all schedule items have been tentatively scheduled (see Figure 2-1) to indicate the required completion dates for the individual tasks thus meeting the shorter schedule.

DEVELOPMENT OF ENERGY DISSIPATING PLASTIC HONEYCOMB
JPL CONTRACT 951172
REVISED SCHEDULE - OCTOBER 24, 1966

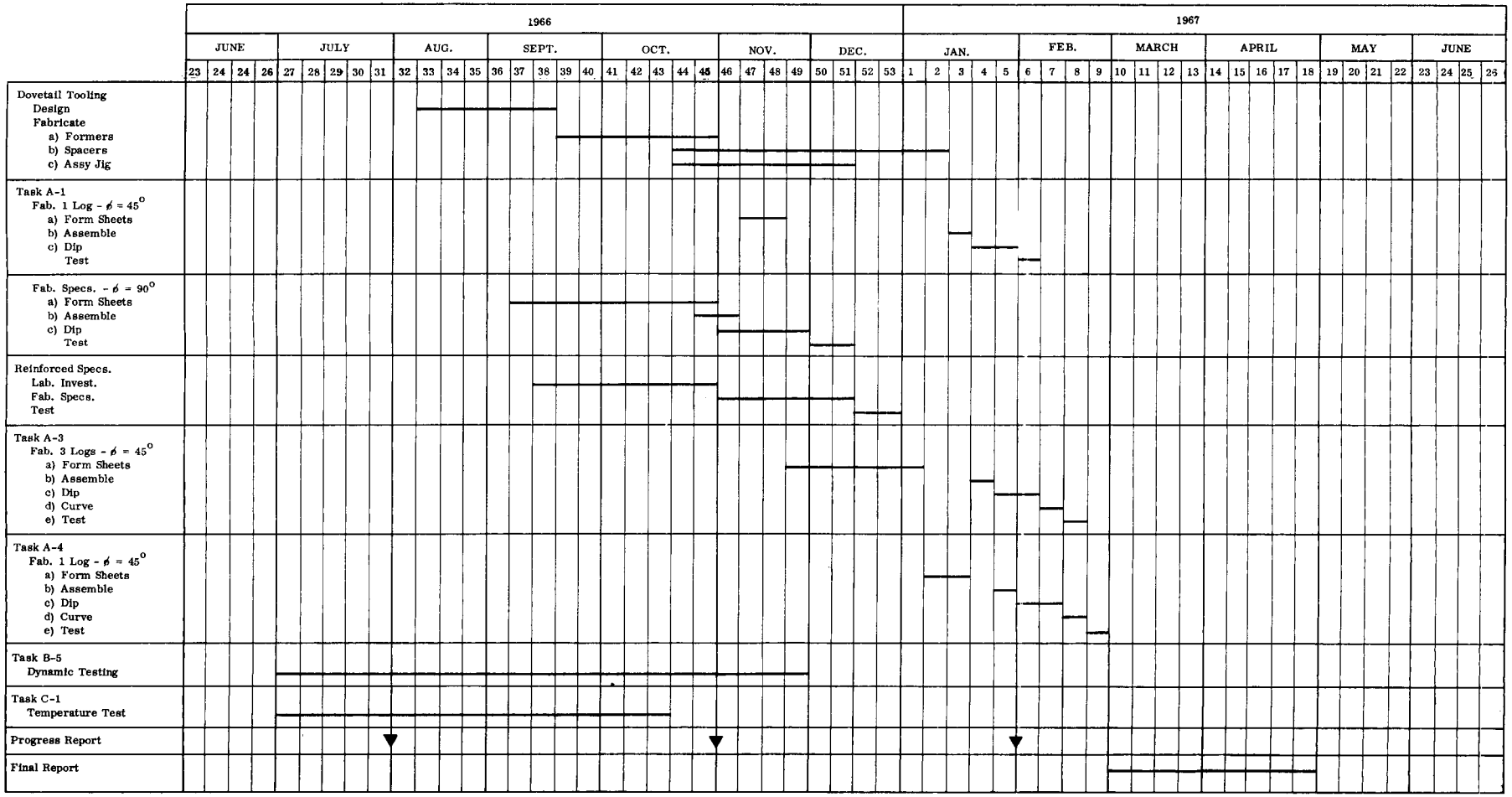

Figure 2-1. Revised Schedule for Development of Energy Dissipating Plastic Honeycomb

SECTION 3

FABRICATION OF DOVETAIL HONEYCOMB

3.1 SMALL SPECIMENS

As discussed in Quarterly Progress Report No. 4, the method of fabricating a satisfactory specimen having a dovetail configuration was established. However, when the fabricated specimens were brought up to density by repeated cycles of dipping and curing, it was noted that the distribution of the dip resin on the cell walls was very poor and voids existed in many areas. Investigation of this problem has shown that the mold release agent, used to prevent sticking of the formers during specimen assembly, is not being removed by the normal cleaning cycle used before the dipping cycle.

In an attempt to eliminate the mold release contamination problem, a different cleaning cycle was used and a different mold release agent was substituted for the existing material. Neither of these changes yielded a suitable solution to the problem. Consequently, to obtain an immediate and definite solution, we decided to coat the metal formers with a teflon material and thereby eliminate the need for any type mold release agent. The formers will be coated and ready for use in the early part of November 1966.

3.2 TOOLING FOR LARGE SPECIMENS (LOGS)

The design of all tooling required to fabricate the large dovetail specimens has been completed, and all long lead time items have been ordered. A set of manufacturing drawings is being forwarded to A. Knoell, JPL Program Technical Monitor, under separate cover. Tooling will enable the fabrication of a log of material 20 inch x 20 inch x 10 inch. Because of chemical process limitations, the log will be constructed from four built-up sections of material joined together before curing of the node bond line adhesive.

To prevent any problems from occurring from the use of mold release agents, plastic formers will be used in the assembly fixture. The material from which these formers are fabricated has an aluminum additive which improves the thermal conductivity of the material. This improved thermal conductivity is required to ensure proper heat transfer through the built-up log during curing of the node bond line adhesive material.

Tooling fixtures are designed to permit dovetail cell configuration changes at a later date, if desired, with only minor modifications being required.

SECTION 4

CURVING INVESTIGATION

4.1 FORMING TECHNIQUES

Two basic types of curving techniques which have been considered for the application of curving plastic honeycomb specimens are as follows:

a. Wraparound former

b. Radial load former

These methods are discussed in the following sections, and the recommended method is described and illustrated.

4.1.1 WRAPAROUND FORMER

The wraparound former and the radial-load former (discussed below) are the most versatile and simple methods of forming honeycomb specimens. The basic objective employed in these two methods is to impose a uniform radial force on the specimen in such a way that little or no bending forces are placed on the specimen. This effect is accomplished by using forces which are applied parallel to edge of the specimen being curved during the entire curving operation. The following series of sketches show how the force (F) is applied, and the resulting radial load (f) on the specimen. The progressive radial load curves the specimen.

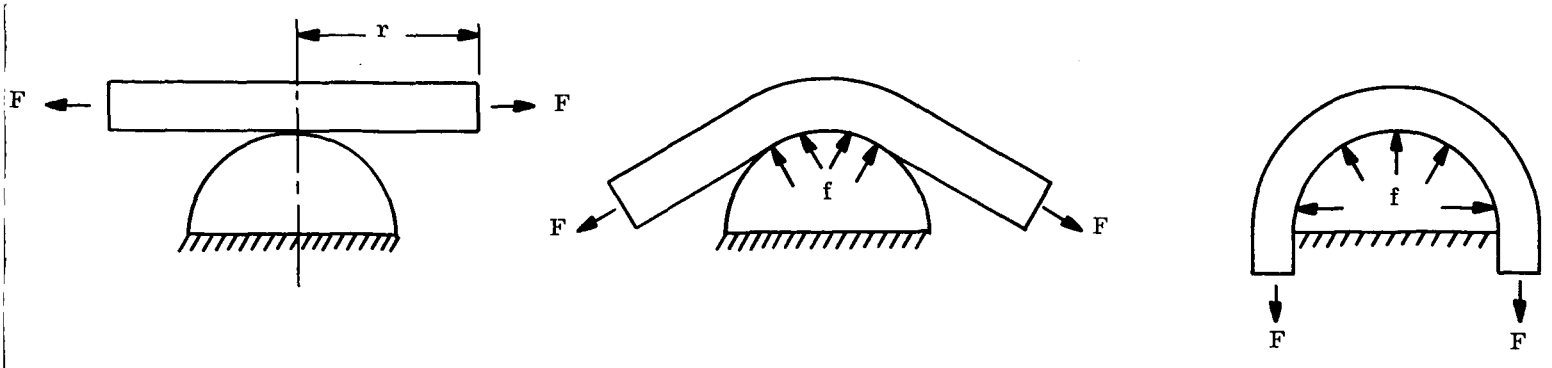

Changes in the value of F around the periphery of the specimen may be required to account for the orthotropic characteristic of the honeycomb. (These changes are easily accomplished and will be explained later.) This type loading may be compared with that found in a spherical pressure vessel, where f is the pressure load and F is the skin tension. In the case of curving, F is the load being applied rather than f. By varying the force F, it is possible to control the expansion or compression of the cells on the inside radius to obtain the desired cell configuration. F can be any value which will result in curving of the specimen, and which has an upper limit of that load which either fails the honeycomb in tension at the node bonds, or causes the honeycomb cell walls to deform due to the radial load f. The tensile strength of the node bond lines will most likely be the limiting factor.

Once one or two different specimen configurations have been curved, it should be possible to calculate the required forces F for other configurations, assuming the same honeycomb type is used. Different honeycomb densities may or may not require a practice run.

4.1.2 RADIAL-LOAD FORMER

This method is the same as the wraparound method with the exception that the forces F are not applied to the specimen being curved but rather to pie-shaped pieces of material placed atop the specimen to be curved. With this method, the only load applied to the specimen is the radial loads f. Therefore, the only restirction is to limit the load F so as not to exceed the crushing stress of the specimen in the direction of the loads f.

A potential problem with this method could be the friction load developed between the pie-shaped pieces of material and the specimen which could prevent the cells of the specimen from properly expanding. However, this type forming has been successfully used in curving plastic honeycomb specimens (see Figure 4-1).

4.1.3 CONCLUSIONS

With the fixture described in Section 4.2, both the wraparound and radial-load methods can be used. The wraparound method will be used first because it is the most flexible and offers the most control of the process.

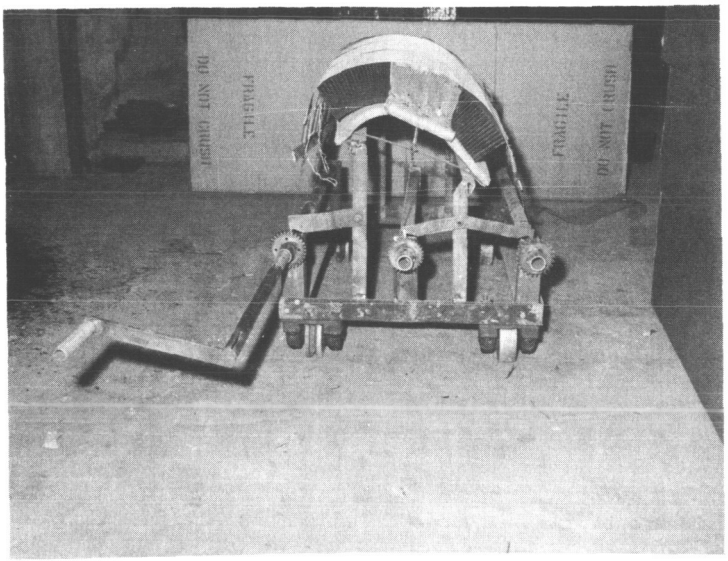

Figure 4-1. Curving of Plastic Honeycomb Specimen by Radial-Load Former Method

4.2 FORMING FIXTURE

The forces F are applied by use of weights around the periphery. These forces are infinitely variable because the weights consist of containers into which lead shot is placed. The rate of curving is controlled by restraining and movement of the weights with the cables shown. These cables are joined in front of the fixture on a bar. Movement of this bar will be controlled by an external source. The use of this fixture will permit measured amounts of lead shot to be added to each container in increments until the proper amount of curving takes place.

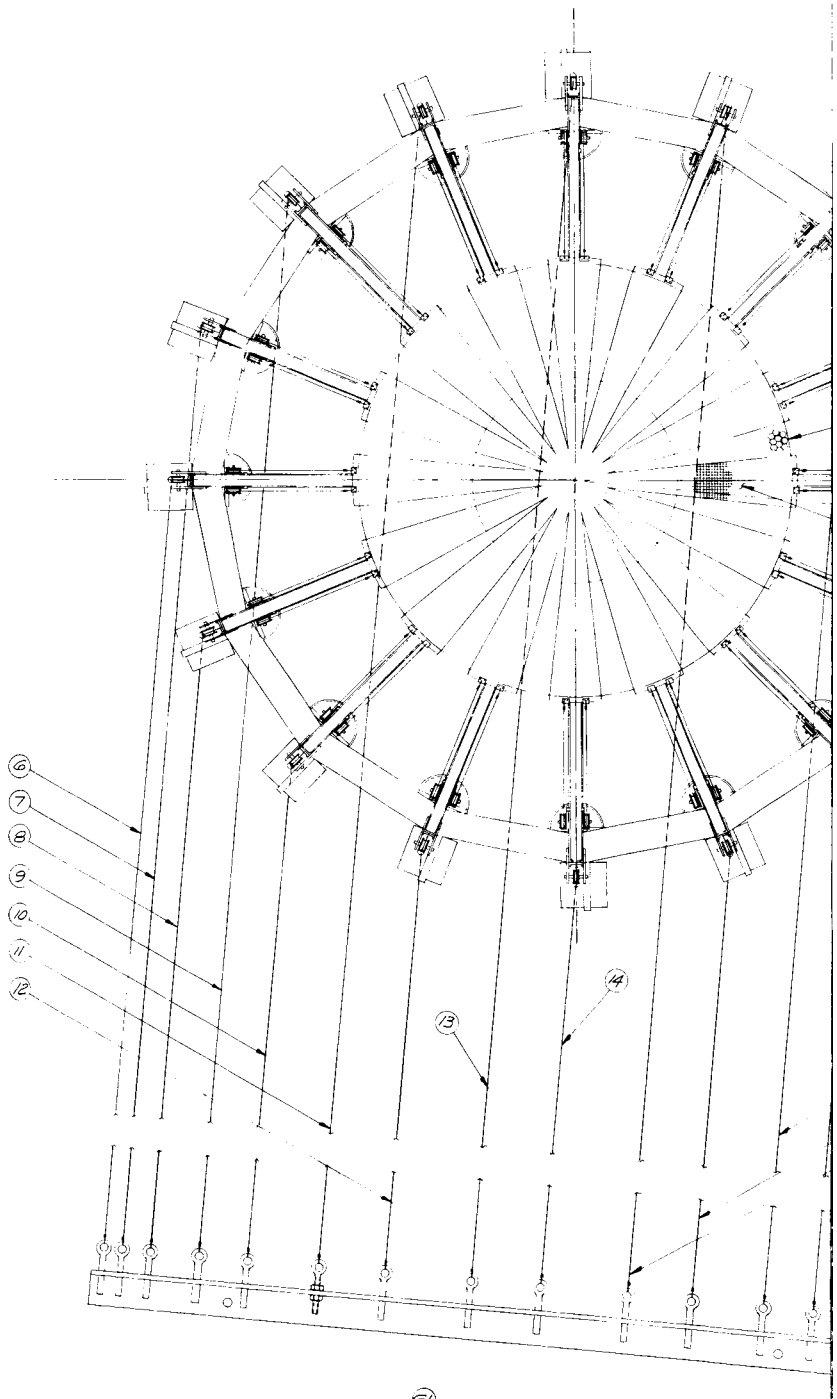

(61)
PLAN VIEW

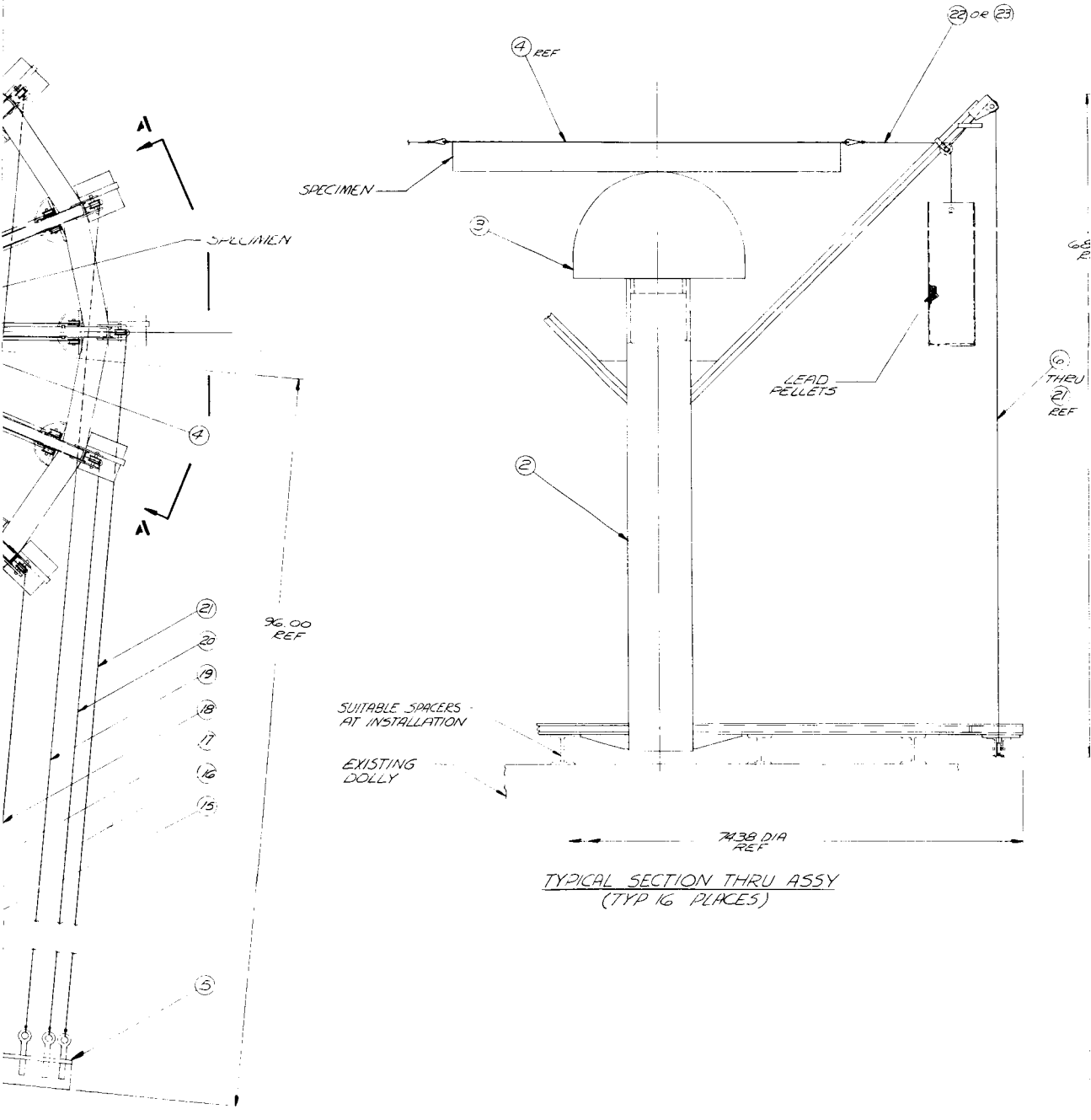

TYPICAL SECTION THRU ASSY
(TYP 16 PLACES)

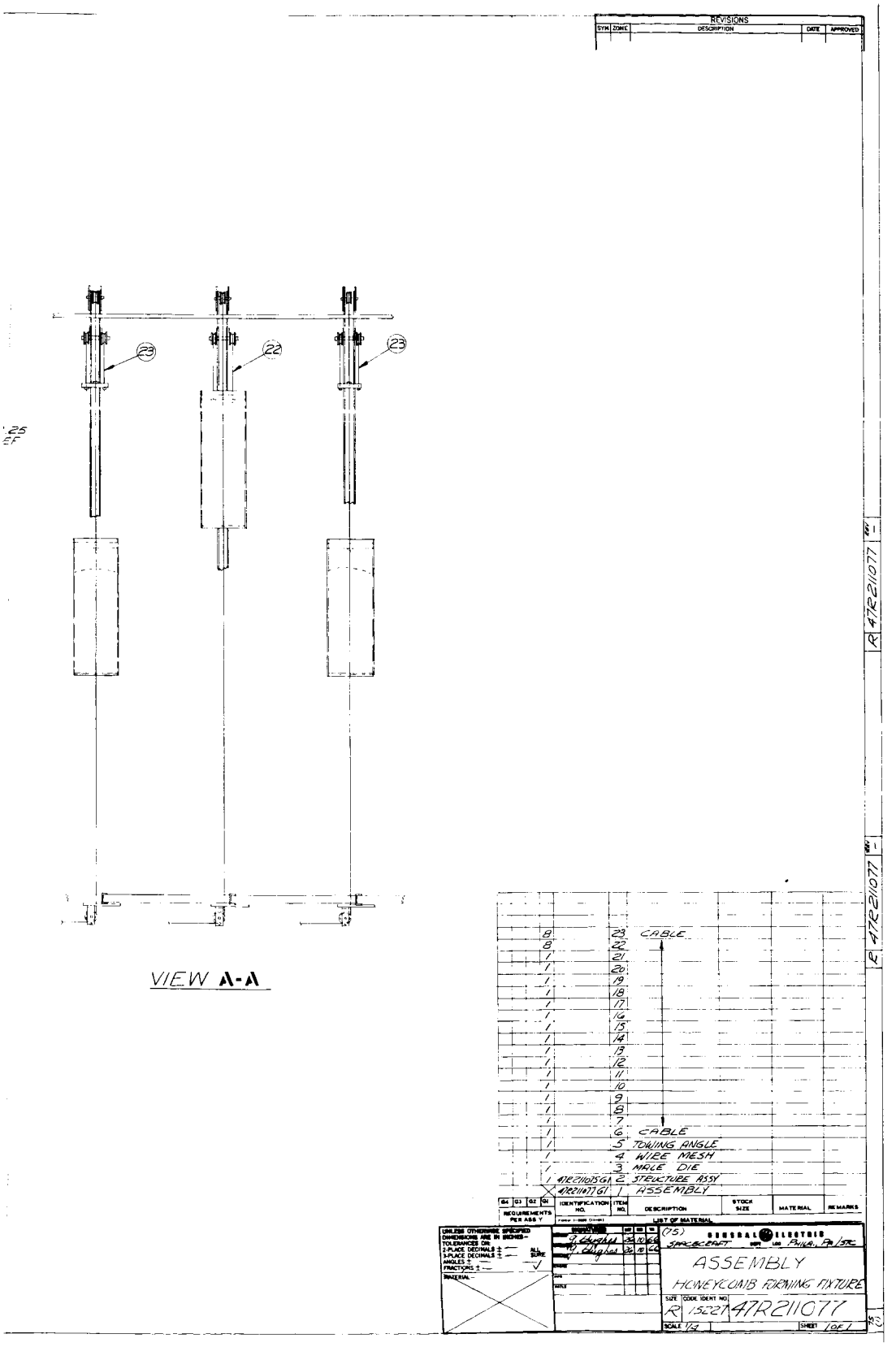

Figure 4-2. Forming Fixture Assembly

SECTION 5

FILLED RESIN INVESTIGATION

5.1 SUMMARY

The investigation of the addition of filler material to the dip resin, as discussed in Paragraph 2.1, has been initiated. The laboratory investigations are almost complete.

The study thus far has shown that it is feasible to modify the existing dip resin with either short fibers or flakes of glass. Sedimentation of the glass is not serious because it can be redispersed by stirring. The remainder of the laboratory investigation will include taking photomicrographs of the coated specimens made thus far and the dipping of additional honeycomb specimens to demonstrate further the process feasibility.

Following completion of the laboratory investigation, specimens to be used for static testing will be fabricated at the honeycomb manufacturer's plant. This effort will be initiated in November 1966.

5.2 DISCUSSION

The presently used phenolic dip resin was modified by adding short glass fibers and glass flakes. Viscosity measurements were made using varying loadings of the additives. The glass fibers, obtained from Owens Corning Fiberglass, were 1/16-inch fibers with a 701 (water) finish, and 1/32-inch fibers with a 709 (cationic) finish. Flake sizes were 2.5 and 3.5 microns.

Viscosity determinations were made by first weighing 350 grams of resin in a container making the determination, then adding incremental quantitities of filler until 90 grams of filler had been added or until a large increase in viscosity was noted. Table 5-1 shows these results. The results are plotted in Figures 5-1 through 5-4. Because the viscosity-increasing characteristics of the 1/16-inch fiber are much greater than the 1/32-inch fiber, the 1/16-inch fiber is not to be considered further.

To evaluate the coating properties of the modified resin, the following specimens were prepared.

Strips of honeycomb prepreg material were cured at 250°F for 1 hour, cut into 1-inch by 6-inch strips, and dipped into resins containing 1/32-inch fibers, 3.5 micron flakes, and 2.5 micron flakes. All three solutions were diluted to 2000 centipoises. Each strip was dipped four times and dried for 15 minutes at 250°F between each dip. The 1/32-inch fiber and 3.5-micron flake solutions covered the strips evenly while the 2.5-micron flake solution yielded uneven and lumpy coatings.

Additional strips were dipped and dried, as described above, into the 1/32-inch fiber, and 3.5-micron flake modified resins. In these dippings the solutions were diluted to 100 centipoises and more evenly coated specimens were obtained. Four specimens made from undipped honeycomb core material were dipped into the two best solutions obtained from the strip tests. These two types of additives, the 1/32-inch fibers and the 3.5-micron flakes, will be used for all further testing. In all four cases, the coating was unsatisfactory. This unsatisfactory condition resulted from insufficient thinning of the resin solution, and an uncontrollable removal rate of the specimen from the solution. On the next specimens, thinner solutions will be used and an optimum dilution determined. The withdrawal rate, which is very difficult to control by hand, will not be a problem when the specimens are fabricated at the manufacturers plant using automated equipment.

Samples of the 1/32-inch fiber and 3.5-micron flake modified resins diluted to 100 centipoises were placed in test tubes to observe sedimentation. The fillers settled approximately 1 inch in a four-inch depth after 24 hours. This settling will cause no problem because the filler is easily redispersed by stirring.

Table 5-1. Viscosity of Resin Upon Filter Addition (Centipoise)

Viscosity without filler: 2300, 2350, 2300				
Wt. of Filler Added to 350 Grams of Resin (Grams)	1/16 in Fibers	1/32 in Fibers	3.5 Microfibers	2.5 Microfibers
0.7	2450. 2500. 2500.	2300. 2350. 2350.	2300. 2300. 2350.	2300. 2300. 2300.
3.7	2500. 2450. 2500.	2400. 2450. 2500.	2400. 2400. 2400.	2400. 2400. 2400.
7.2	2700. 2650. 2700.	2450. 2500. 2500.	2550. 2550. 2600.	2500. 2500. 2550.
14.2	3300. 3300. 3300.	3200. 3150. 3250.	3150. 3150. 3150.	2750. 2750. 2750.
24.2	4300. 4350. 4350.	3550. 3550. 3550.	3900. 3900. 3900.	3500. 3550. 3550.
30.0	4900. 4800. 4850.	3600. 3650. 3700.	4250. 4250. 4300.	3900. 4000. 4000.
45.0	11,200. 10,900. 10,900.	4100. 4100. 4100.	6400. 6400. 6450.	6350. 6350. 6300.
60.0	53,000. 50,000. 50,000.	4400. 4450. 4450.	7950. 7950. 7900.	8250. 8200. 8250.
90.0		6150. 6150. 6150.	15,200. 15,000. 15,000.	

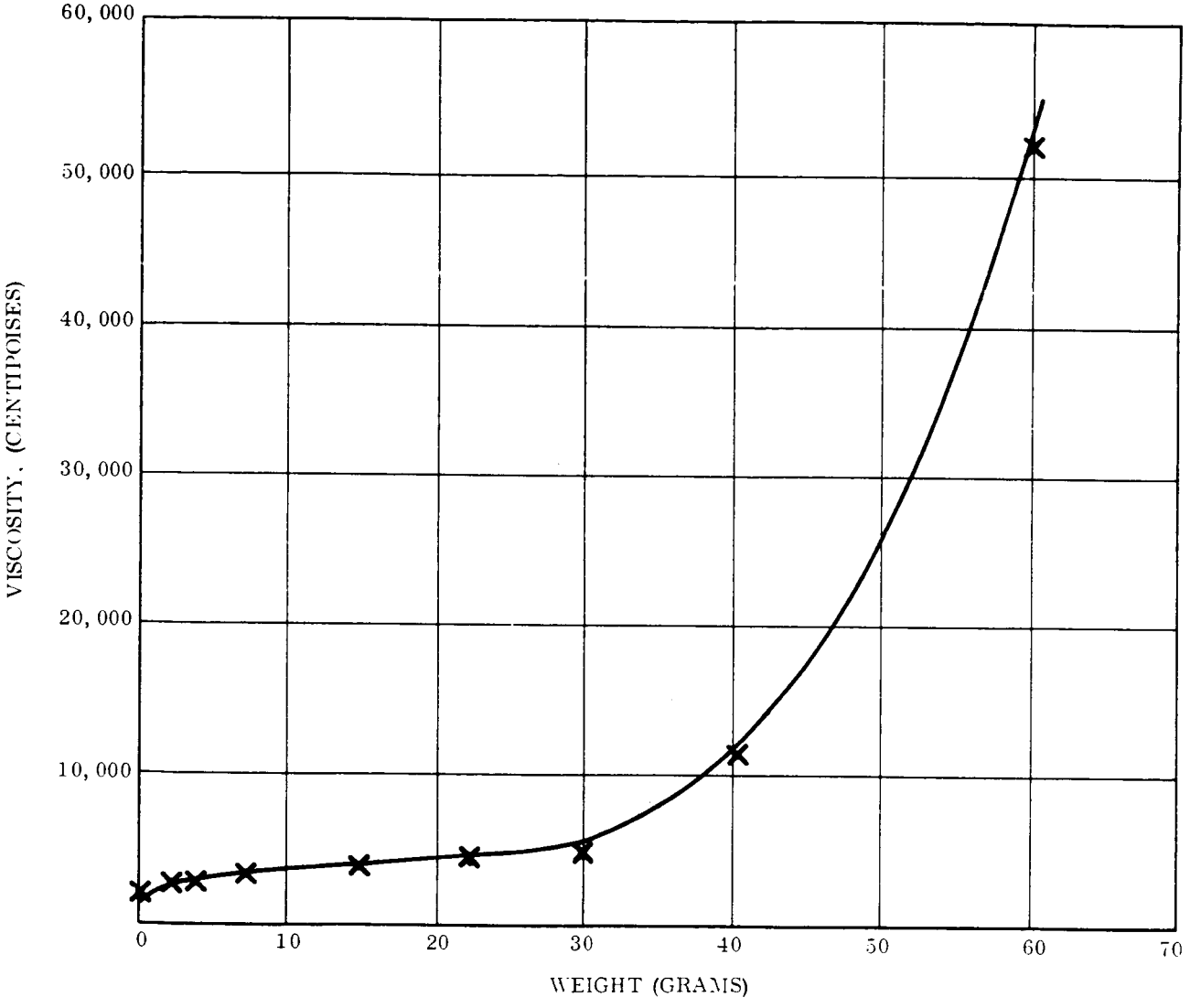

Figure 5-1. Weight of 1/16-Inch Fiberglass Added, 701 Finish

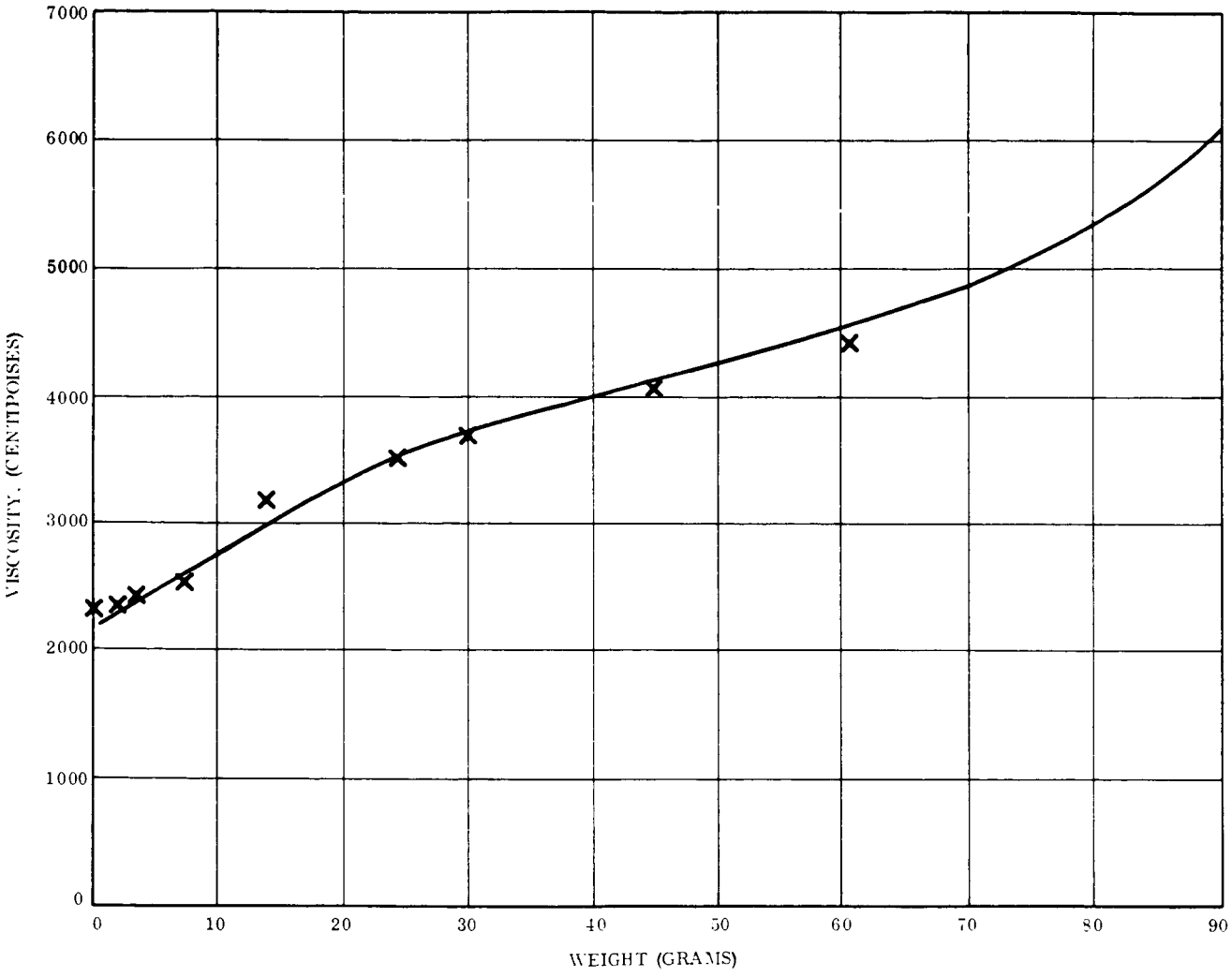

Figure 5-2. Weight of 1/32-Inch Fiberglass Added, 709 Finish

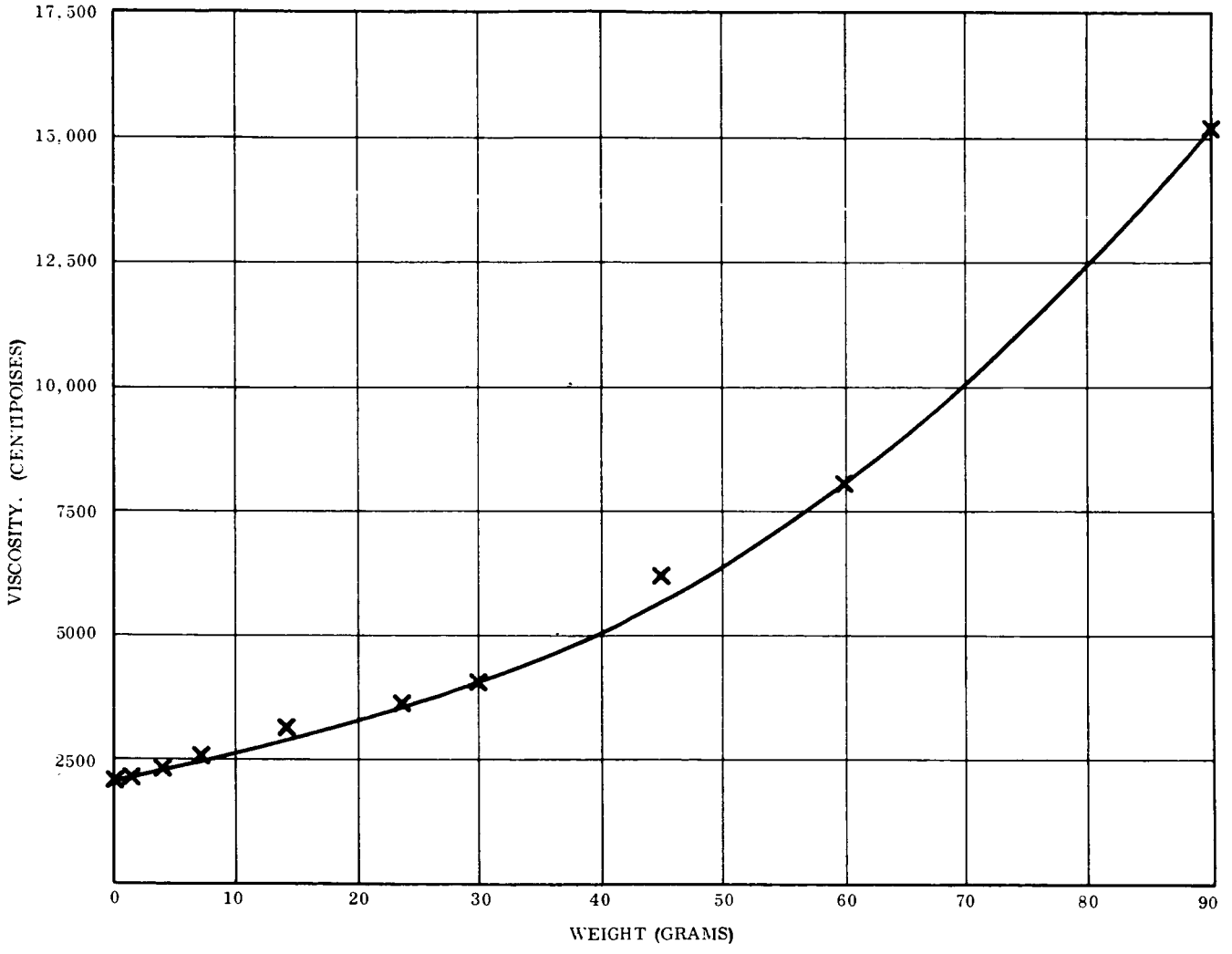

Figure 5-3. Weight of 2.5 M Glass Flakes Added

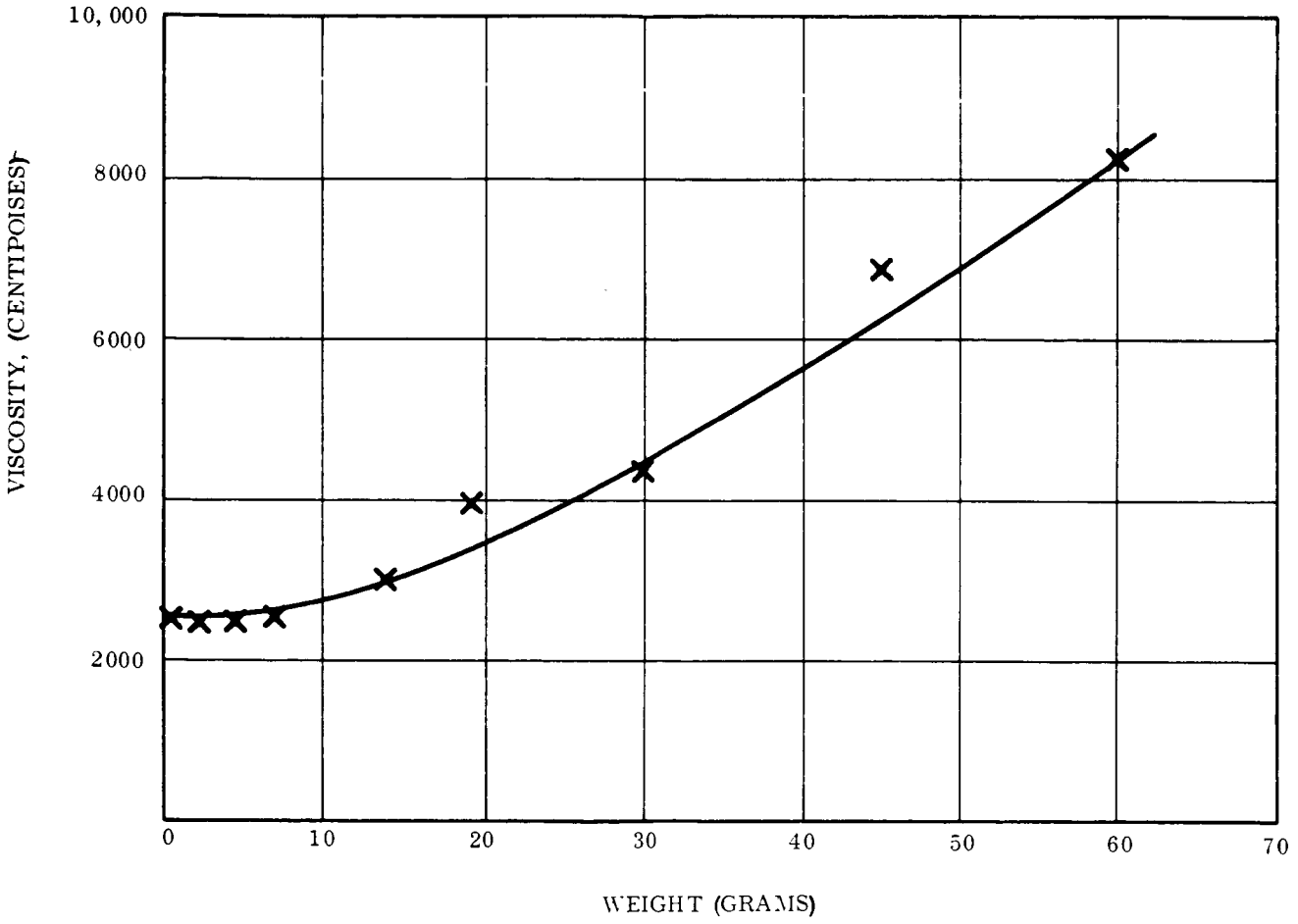

Figure 5-4. Weight of 3.5 M Glass Flakes Added

SECTION 6

TESTING

6.1 DOVETAIL - STATIC TESTS

When tested, the first specimen of hand-formed dovetail honeycomb behaved very poorly. Results of the four specimens tested are shown in Table 6-1. The type of failure or crushing mode observed was very similar to that obtained on light-density specimens tested previously. In this type of crushing mode, the glass fiber bends and breaks off in rather large pieces instead of crumbling into a fine powder. This can be observed in the pictures on Test A-li-a in the Appendix. The problem was therefore diagnosed as one of the final thickness of the cell walls being too thin, and the next three specimens were dipped to a density of approximately 12.5 pounds. Following testing of these three specimens it became apparent as discussed in Section 3.1, that the adhesion of the dip resin to the lay-up, rather than the density of the specimen, was the problem.

6.2 TEMPERATURE TESTS

6.2.1 TESTS AT 200°F

Before the actual tests were performed, sample specimens were exposed to the time and temperature cycles and conditions simulating existing conditions of a static test. Thermocouples were used on the specimens to monitor the temperatures. Test procedure consisted of first heating the specimen and the platens in an air-circulating oven to a temperature of 200°F. Next, specimen and platens where placed on the testing machine. Surrounding the specimen on the machine were heat lamps so located that they maintained the specimen at the desired temperature.

From Table 6-1, data show that each of the four specimens yielded a high crushing stress during the first part of the stroke. As the stroke continued, the material started to fail at the node bond lines around the outside of the specimen and caused the outer cell walls to break off in long pieces and tilt away from the axis of the specimen. When this type failure occurs, the crushing stress reduces in proportion to the remaining area on the specimen formed by the cells which do not tilt. This specimen reaction is typical when

Table 6-1. Tests Results

Description	Test	Principal Steady State Stress (psi)	Density (pcf)	Stroke Efficiency (percent)	Stress to Density Ratio (10^6 in.)	Gross Specific Energy (10^3 ft-lb/lb)	Specific Energy x Stroke Efficiency (10^3 ft-lb/lb)
Hand-formed Dovetail	A-1i-a	289	8.0	-	0.063	5.3	-
	A-1i-b	544	12.6	76	0.075	6.3	4.8
	A-1i-c	550	12.6	70	0.075	6.3	4.4
	A-1i-d	388	12.2	82	0.055	4.6	3.8
Prefailed Edge Shear Tests	B-3-n	78	–	–	Failure Stress Shown Only		–
	B-3-m	110	–	–	–	–	–
200^{o}F Temperature Tests	C-1-d	2620	–	–	–	–	–
	C-1-e	2560	–	–	Principal Steady State Stress Before Failures - See Text		–
	C-1-f	2560	–	–			–
	C-1-g	2470	–	–	–	–	–
-100^{o}F Temperature Tests	C-1-h	2620	12.7	-	0.356	29.8	-
	C-1-i	2720	13.4	See	0.350	29.3	See
	C-1-j	2450	12.8	Text	0.331	27.7	Text
	C-1-k	2400	13.2	-	0.314	26.2	-

relatively weak node bond lines exist. The conclusion is therefore, that the effective strength of the node bond lines decreases much more rapidly with increasing temperature than does the strength of the dip resin.

This drop off in crushing stress would probably not occur if a penetration-type test were performed. Also, this reduction of strength in the node bond lines would undoubtedly adversely affect the performance of the material in a curved specimen where, on part of the specimen, forces are directly applied on an axis not parallel to the cell axis.

6.2.2 TESTS AT -100°F

As can be seen in Table 6-1 the tests results of specimens C-1-h through C-1-k, show that the material behaved very well and yielded high values of specific energy absorption. The values of stroke efficiency were not calculated for these specimens because an interference occurred between the dry ice and platens. This interference caused the apparent crushing value to increase sooner than expected. Based on the orderliness of crushing and the fine powder resulting from the crushing, it is reasonable to assume that the stroke efficiency would be equal to that obtained on the same type specimen at room temperature.

Test procedure for specimens tested at -100°F was similar to that used for the elevated temperature tests. The specimens and platens were (1) placed in a cold oven, (2) removed and placed on the testing machine, and (3) surrounded by dry ice. Although not originally anticipated, this arrangement on the machine yielded a steady state specimen temperature of -94°F when the specimen was placed on the test machine. The temperature was independent of the length of time that the specimen was left in this position. Tests were therefore performed at this temperature.

6.3 HIGH VELOCITY TESTS

Of thirteen tests performed in the high velocity range, seven yielded sufficient data to permit a quantitative evaluation of material performance. Ten of these thirteen tests were conducted at a nominal impact velocity of 500 fps and three at 250 fps. In all tests, the specimens were loaded satisfactorily, with excellent parallelism between projectile and specimen impact surfaces being maintained throughout the entire process. Based on the

post-impact inspection of the test chamber, all specimens fragmented into small pieces and in all cases no portion of the specimens was found attached to the mounting fixture. This specimen reaction was attributed to the fact that bottoming occurred in every test with further compression displacement being maintained between the projectile and specimen mounting fixture. High speed motion pictures showed that mass dispersion of the crushed material occurred during the bottoming displacement interval. During the crushing process, however, fragmentation occurred only at the local boundaries.

6.3.1 RESULTS AND DISCUSSION

Data obtained from the tests are listed in Table 6-2.

Table 6-2. High Velocity Test Results

Test No.	Spec. Type	V_o (fps)	L. P. Level (KH_g)	$\bar{\sigma}$ (psi)	W (gm)	(ft-lb/lb)
B-5-a	A	468	--	2600	172.1	20,600
B-5-b	A	429	--	800	169.8	6,000
B-5-c	A	423	--	3200	169.4	24,300
B-5-d	B	262	--	2840	179.1	21,600
B-5-e	B	255	--	2860	168.7	21,800
B-5-f	B	258(1)	3	3340	170.1	25,400
B-5-g	B	462	3	5150	169.1	39,400

(1) estimated.
Type A - Thin dipped with improved bond - 14 PCF
Type B - Thin dipped - 14 PCF
Specimen Size - 3.5 x 3.5 x 4.0 inch

The specific energy, K_e, was calculated according to the formula:

$$K_e = \frac{\bar{\sigma}}{\rho\omega}\,\beta \qquad (1)$$

where $\bar{\sigma}$ is the average stress during crushing, ρ_ω the weight density of the specimen, and β, the stroke efficiency, assigned a value of 0.70. Values of $\bar{\sigma}$ for Test Nos. B-5-a, B-5-b, B-5-c and B-5-d were obtained from Fastax film measurements, whereas the remainder were derived from accelerometer data.

Values of K_e, but for two exceptions, range between 20,600 and 25,400 lb/lb, significantly higher than the static value. The low specific energy obtained from Test No. B-5-b may possibly be explained by specimen malfunction because the high speed photographs indicate what could be interpreted as a crack in the specimen body. The evidence is not conclusive, however, and further tests should be done to clarify this point. Even more surprising are the results from Test No. B-5-g which show an average crushing stress of almost twice the static value. This result is expected to be clarified when the results of the last two tests, yet to be performed at a similar impact velocity, become available.

6.3.2 TEST RECORDS

Pertinent data which form the basis of the above mentioned results are displayed in Figures 6-1 to 6-5. Figure 6-1 shows the measurements of projectile displacement, S, as a function of frame number. The interval covered corresponds to an essentially constant frame rate of 14,600 fps. The plot is, therefore, of displacement vs. time. The displacement is referred to the position occupied by the impacted surface of the specimen and, hence, the zero displacement value corresponds to the time of initial impact. The test interval is, therefore, that portion of the displacement curve between S = 0 and 3.0 inches, assuming a value of stroke efficiency equal to 0.75.

A parabola was fit to this curve at the following points: S - 0, t = 0 frames S = 2.20 inches, t = 11.1 frames, and S = 3 inches, t = 16 frames, which are indicated by the squared dots in Figure 6-1. The parabola is defined by Equation (2).

$$t = 4.500\ S + 0.2778\ S^2 \qquad (2)$$

with the time, t, in the unit of frame number (1 frame number corresponds to $\frac{1}{14,600}$ = 68.5μsec.). From this the velocity equation is

$$V = \frac{dS}{dt} = \frac{1}{4.500 + 0.5556S} \qquad (3)$$

For S = 0 and 3.0 inches, the velocities are 270 and 197 fps. respectively, or a velocity change of 73 fps. Hence, the average deceleration during this interval is

$$a = \frac{\Delta V}{\Delta t} = \frac{73}{16} \frac{(14,600)}{(32.16)} = 2071 \text{ g}$$

From this, the average stress is obtained.

$$\bar{\sigma} = \frac{\bar{a} W_p}{A} = \frac{2071 (7608)}{(3.5)^2 (453.6)} = 2840 \text{ psi}$$

where W_p is the projectile weight and A the specimen cross-section area. Using Equation (1), the value of specific energy is:

$$K_e = \frac{2840 (0.75)}{0.0076 (12)} = 23,200 \text{ ft.}$$

The initial velocity of the projectile as obtained from the slope of the displacement-time variation before impact was 262 fps as compared with 270 fps which is the velocity indicated from the curve fit at S = 0. The velocity difference obtained from the terminal points of the parabola, however, was considered to be the consistant basis for determining the average deceleration during the interval S = 0 to S = 3.0 inches.

Accelerometer records obtained from Test Numbers B-5-e, B-5-f and B-5-g are shown in Figures 6-2 and 6-4 inclusive. Two records are shown in each figure. Records (a) and (b) correspond to low pass filter frequencies of 3 and 6 KHertz, respectively. The records (a) and (b) are consistantly related to each other as can be seen by superimposing the two records of a given test. The times at which bottoming of the projectile on the fully crushed specimen occurs are clearly shown by the suddenly rising portion of the curves and closely

check with expected times calculated from the impact velocity, specimen initial length, and average deceleration value. Detailed discussion of the significance of fluctuations in the deceleration records, which are due to specimen response will be presented later.

2. Drop Test Results

Thus far, one drop test of the thin-dipped type specimen at room temperature has been made. The deceleration record of Test No. B-5-h is shown in Figure 6-5-a. A shift of the zero reference for deceleration is evident during the orderly response in the overrall record. A rectified curve is shown in Figure 6-5-b in which an adjustment of the zero line, based on the obviously uniform deceleration level evident in the record, has been made. The low pass filter frequency utilized in this test was 1 KHertz which represents an approximately similar proportion of filtration to physical pulse frequency as utilized in the high velocity tests. The performance values derrived from these records are as follows:

Average crushing stress: $\bar{\sigma} = 1070$ psi

Specific Energy: $K_e = 8,400$ ft-lb/lb

which includes a stroke efficiency value of 0.75. These values are generally confirmed by the values obtained by using the initial energy and before-and-after length measurements of the specimen.

The data presented in this report summary are subject to revisions that may result from further study.

6.4 SHEAR TESTS - HONEYCOMB PREFAILED EDGE

Specimens were prepared and tested to determine the shear strength of the joint where the prefailed edge of the material is bonded to a substrate simulating a vehicle skin. The material was prefailed as shown in Section 3.3.7, Quarterly Progress Report No. 3. The substrate used was a 1/4 inch-thick aluminum plate. Attachment of the core material to the plate was accomplished using Shell 934 bonding agent.

The test set-up is shown on the test chart for Test B-3-n in the Appendix.

An average shear stress of 94 psi was obtained with these specimens. As can be seen on the tests pictures, the precut area of the material failed in a somewhat random manner at both ends of the material stubs.

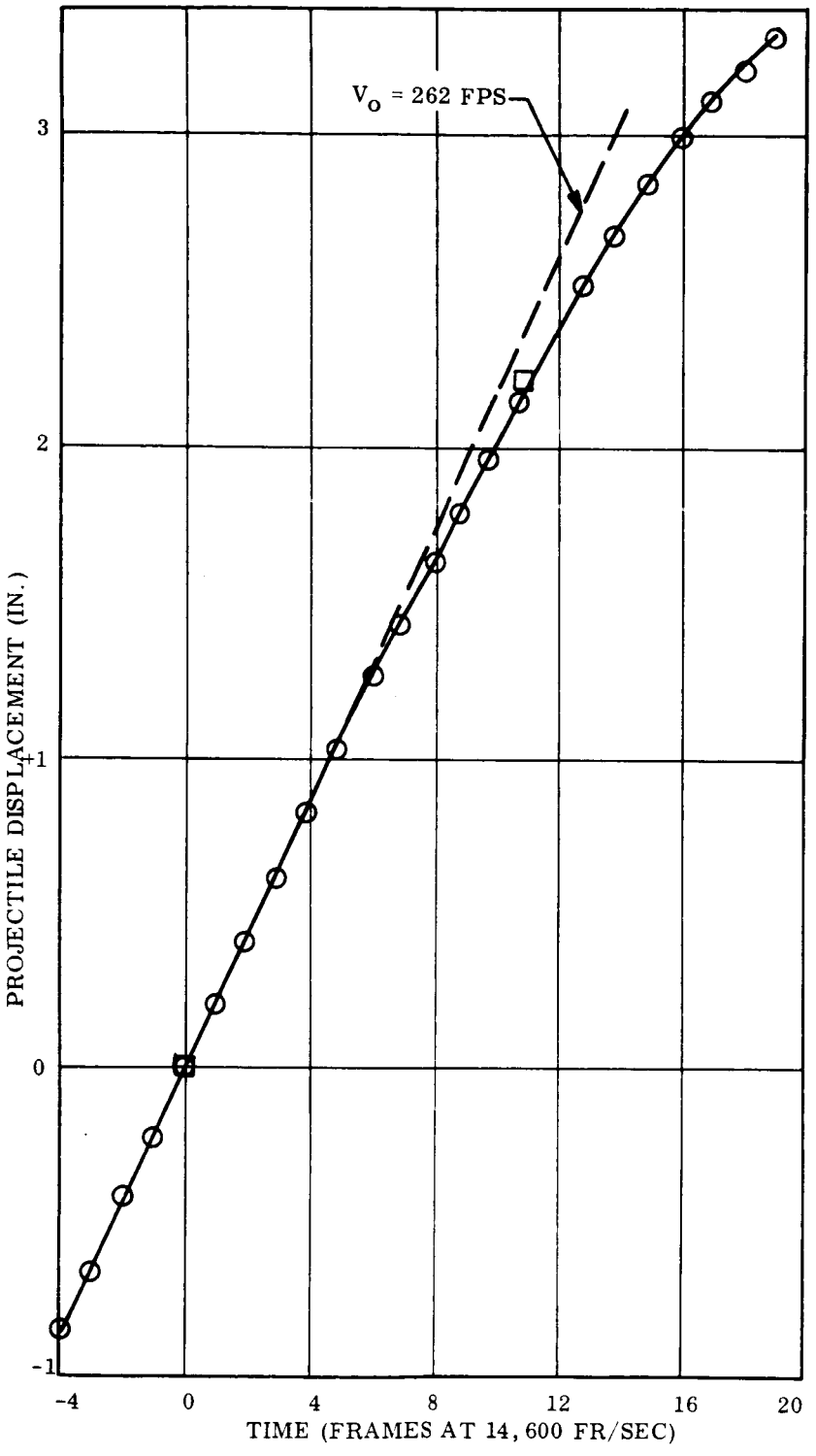

Figure 6-1. Measurements of Projectile Displacement S as A Function of Frame Number

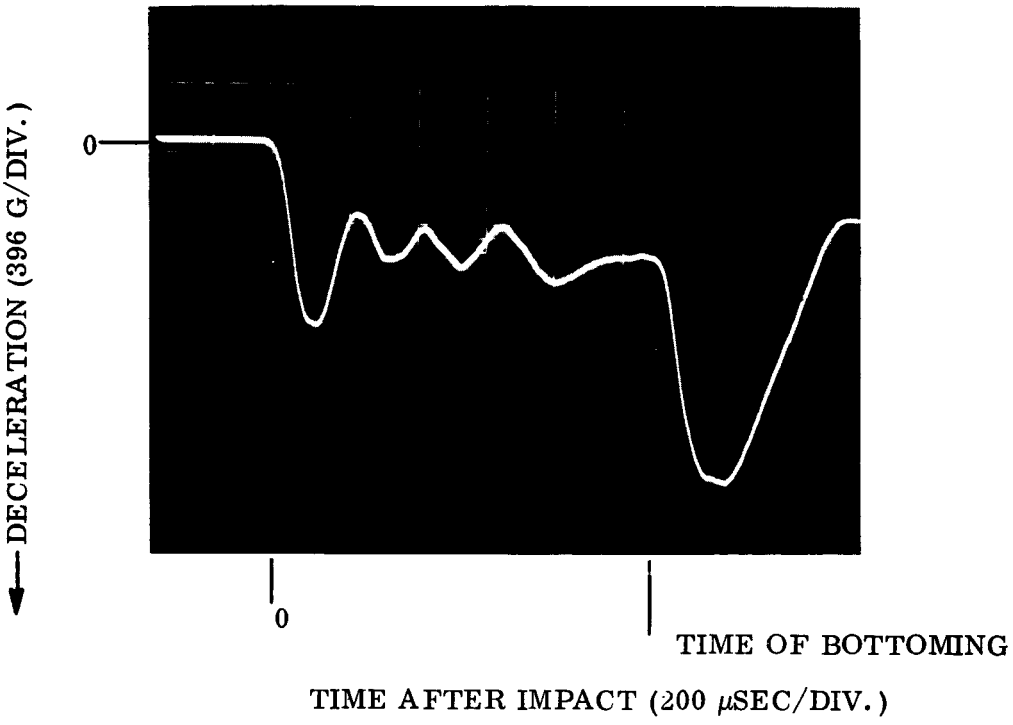

a) 3 KHz L. P.

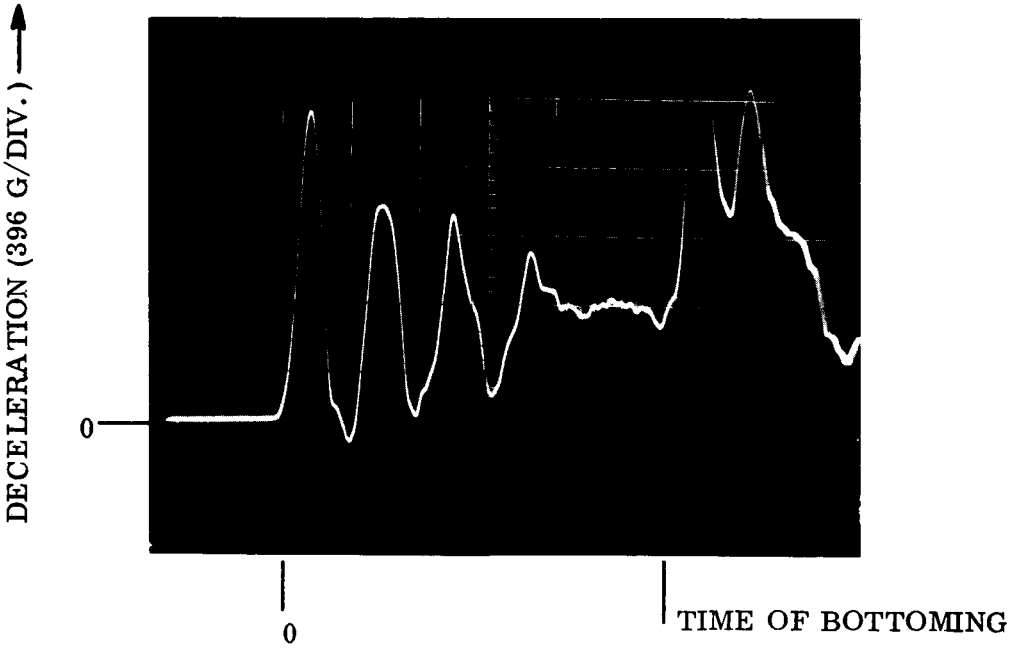

b) 6 KHz L. P.

Figure 6-2. Deceleration Records - Test No. B-5-e

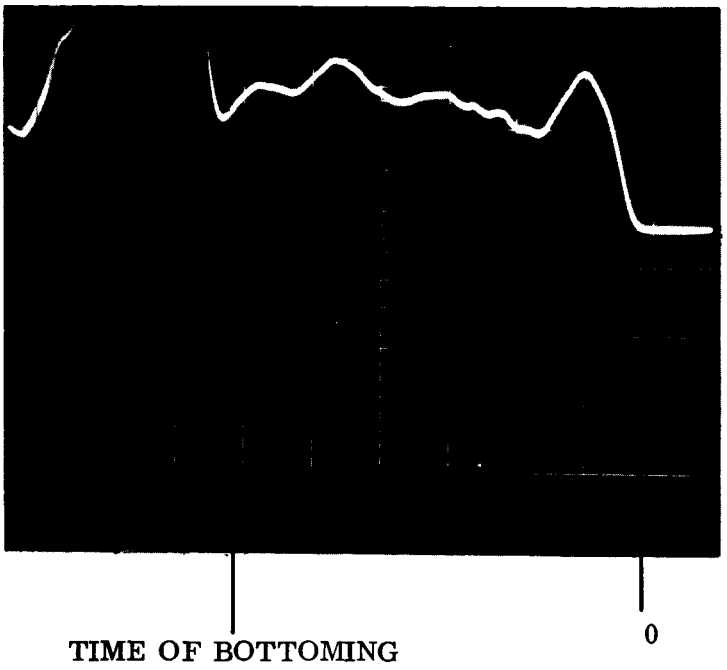

a) 3 KHz L. P.

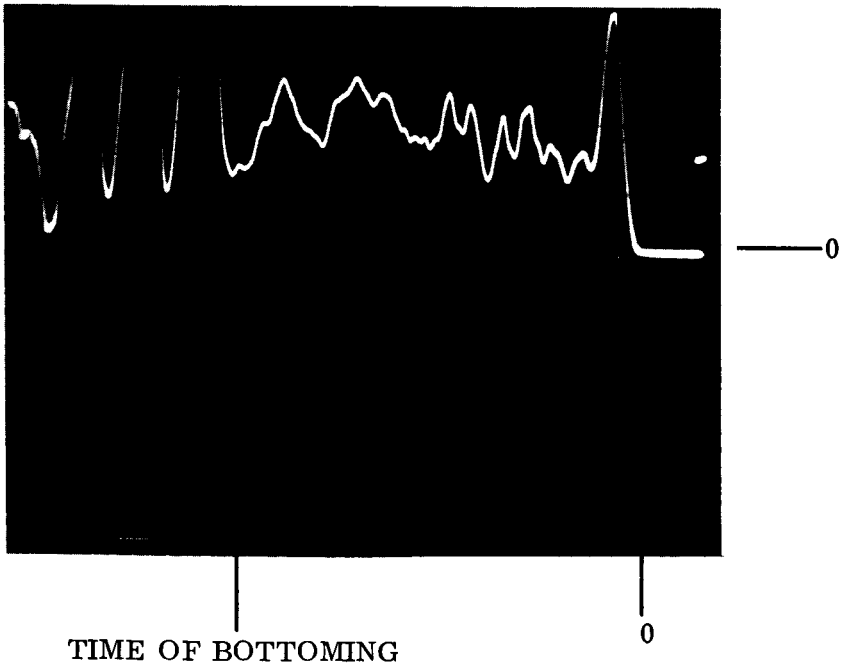

b) 6 KHz L. P.

Figure 6-3. Deceleration Records - Test No. B-5-f

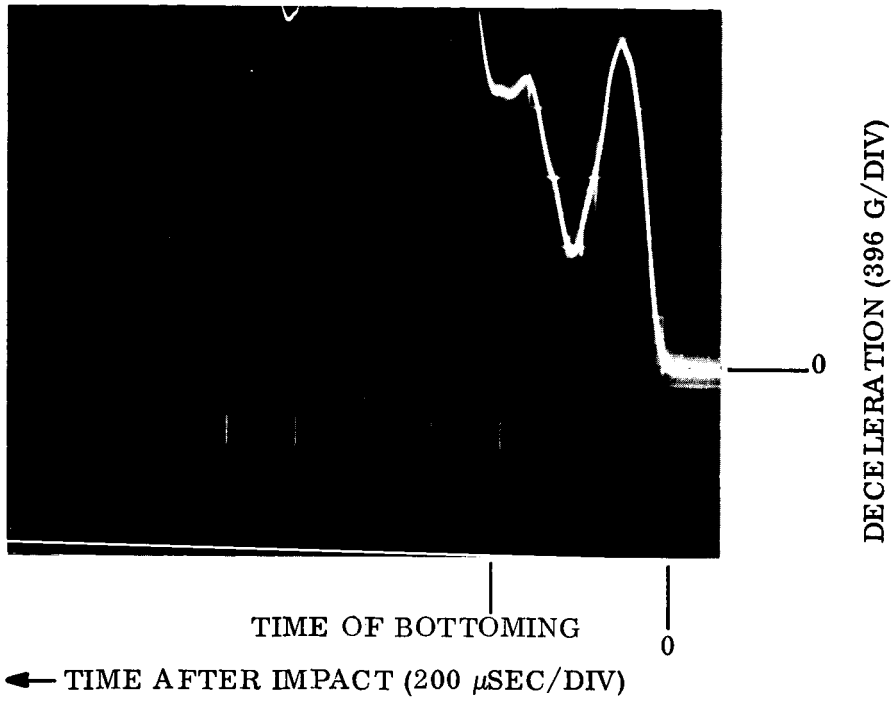

a) 3 KHz L. P.

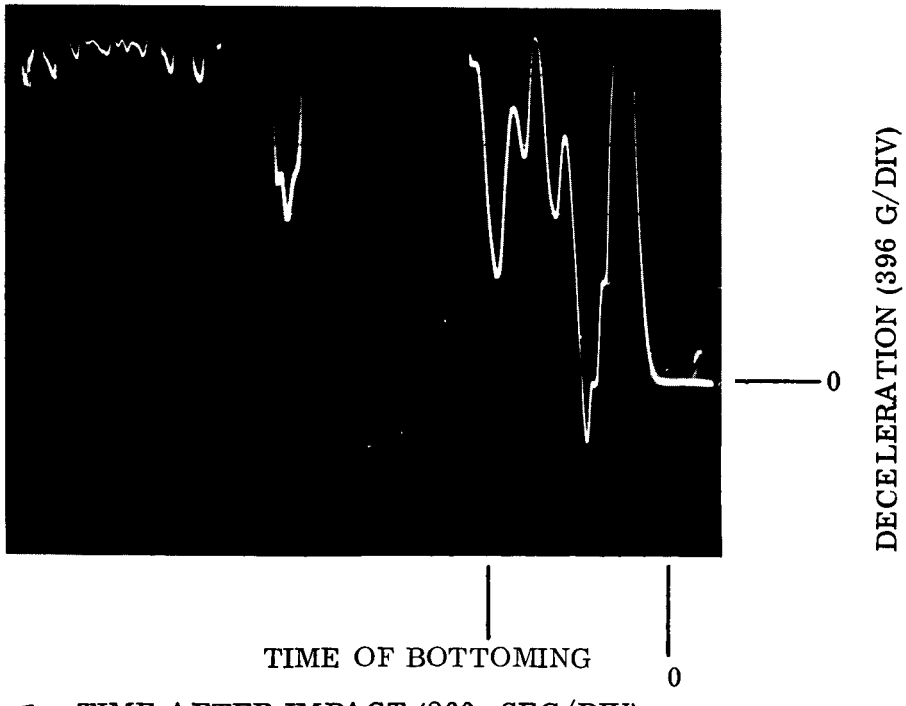

b) 6 KHz L. P.

Figure 6-4. Deceleration Records-Test No. B-5-g

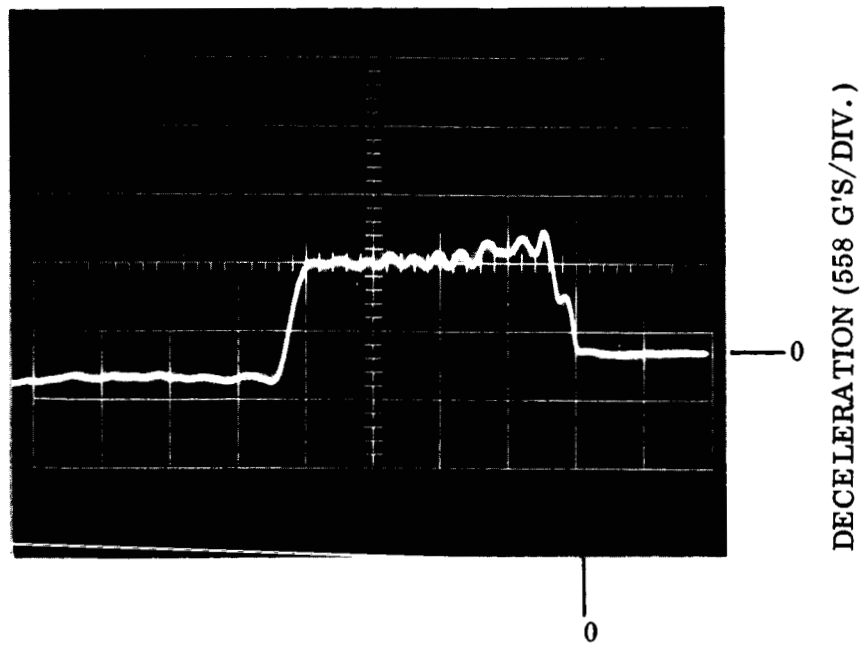

a) ORIGINAL RECORD, 1 KHz L. P., SHOWING AMPLITUDE ZERO SHIFT

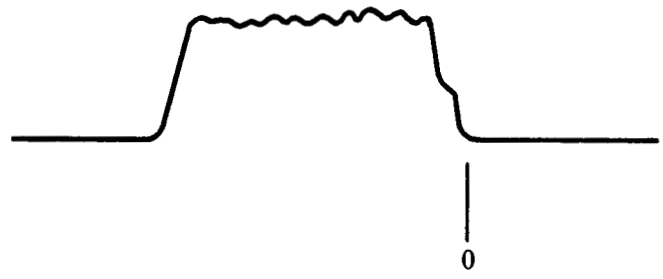

b) RECTIFIED RECORD

Figure 6-5. Deceleration Records - Test No. B-5-h

SECTION 7

ACTUAL VS PLANNED MAN-HOUR UTILIZATION

Figure 7-1 is a graph of actual versus planned man-hour utilization for the period of the contract through October 31, 1966.

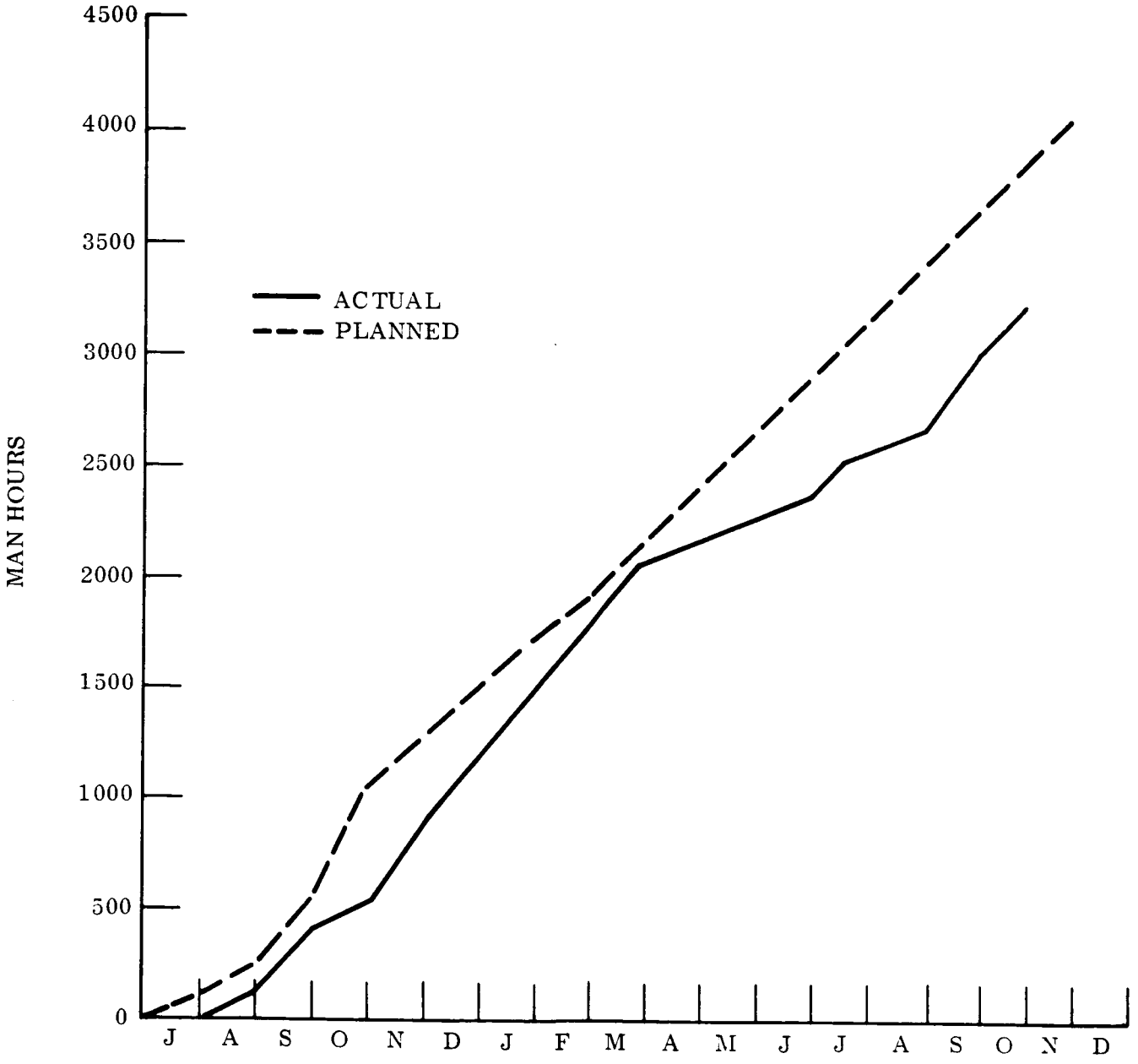

Figure 7-1. Actual vs Planned Man-Hour Utilization

SECTION 8

ANTICIPATED PROBLEMS

No major problems are anticipated. However, the target schedule as presented in Section 2.2 assumes that all tooling will be delivered on schedule and that no major difficulties will be encountered in using these tools. On this basis, while the schedule is realistic, constant surveillance of all items will be required to ensure meeting this target schedule.

SECTION 9

WORK PLANNED FOR NEXT QUARTER

The following work will be performed during the next quarter:

- Procure all tooling required for fabrication of large size dovetail specimens.
- Assemble first dovetail log specimen.
- Complete fabrication and testing of fully expanded cell dovetail specimens.
- Complete investigation of glass filled dip resins.
- Complete dynamic testing on all specimens.

APPENDIX
TESTS GRAPHS

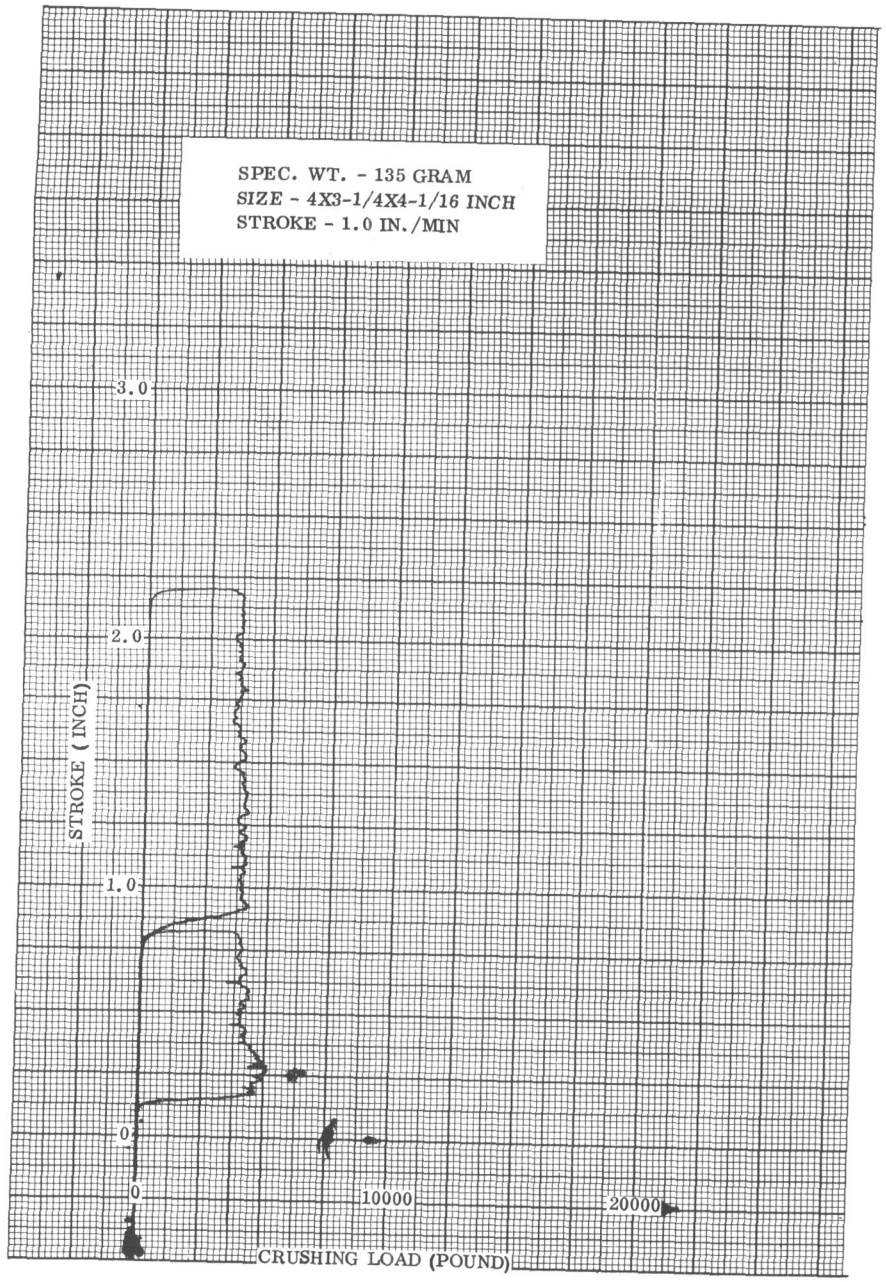

Test A-1i-a - Dovetail - 11 pcf

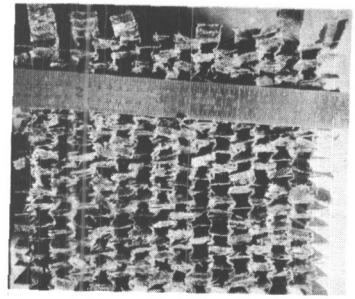

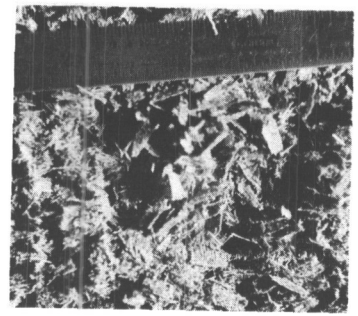

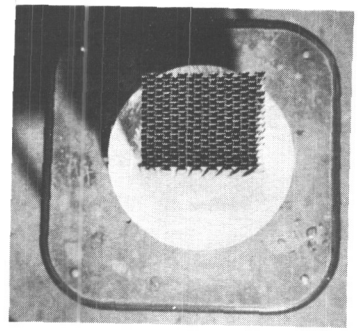

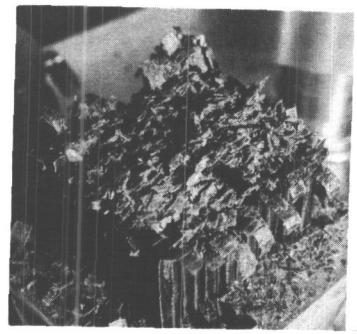

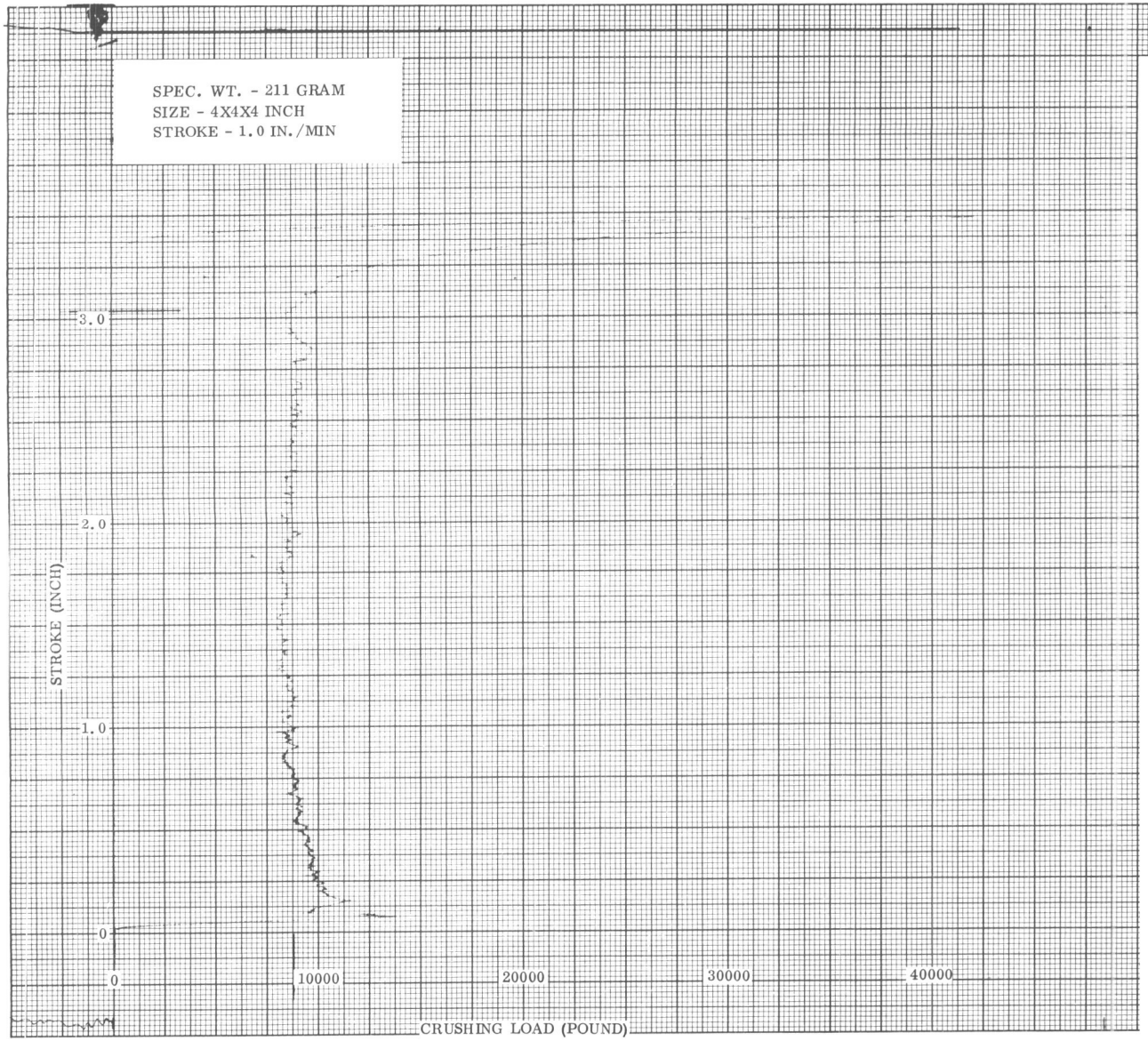

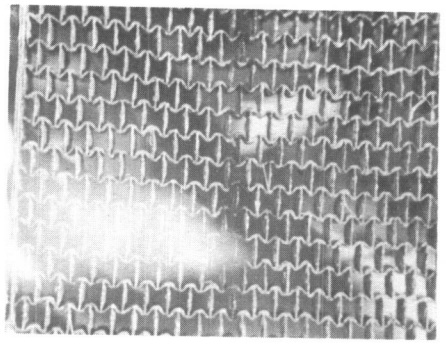

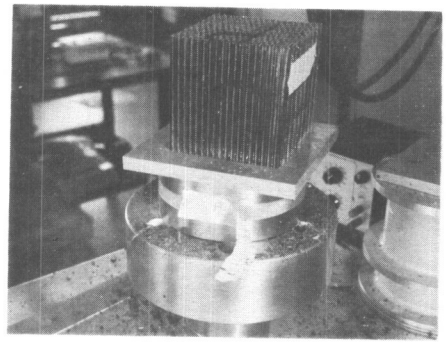

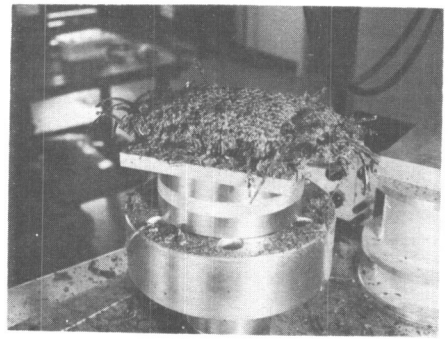

Test A-1i-b - Dovetail - 14 pcf

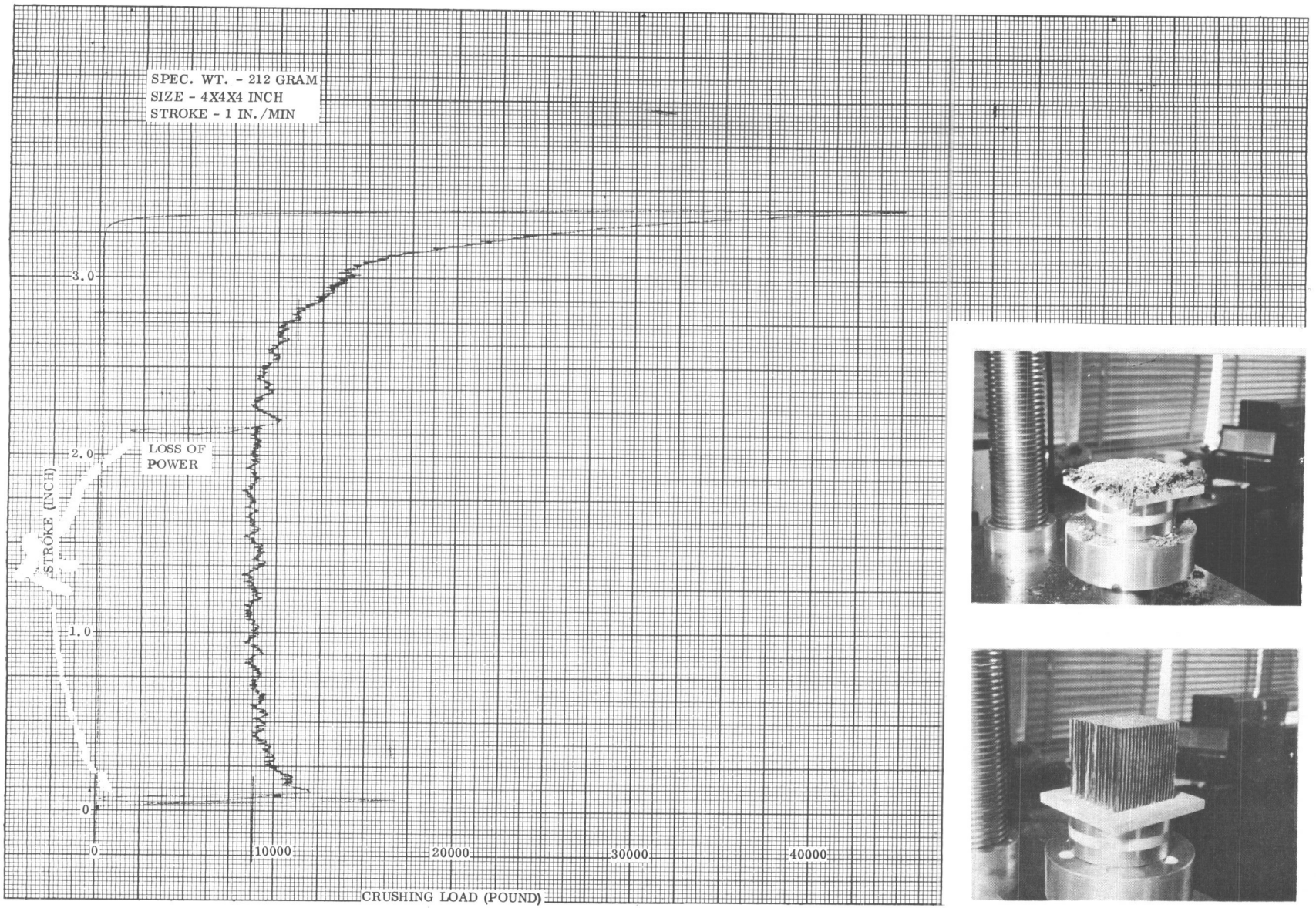

Test A-1i-c - Dovetail - 14 pcf

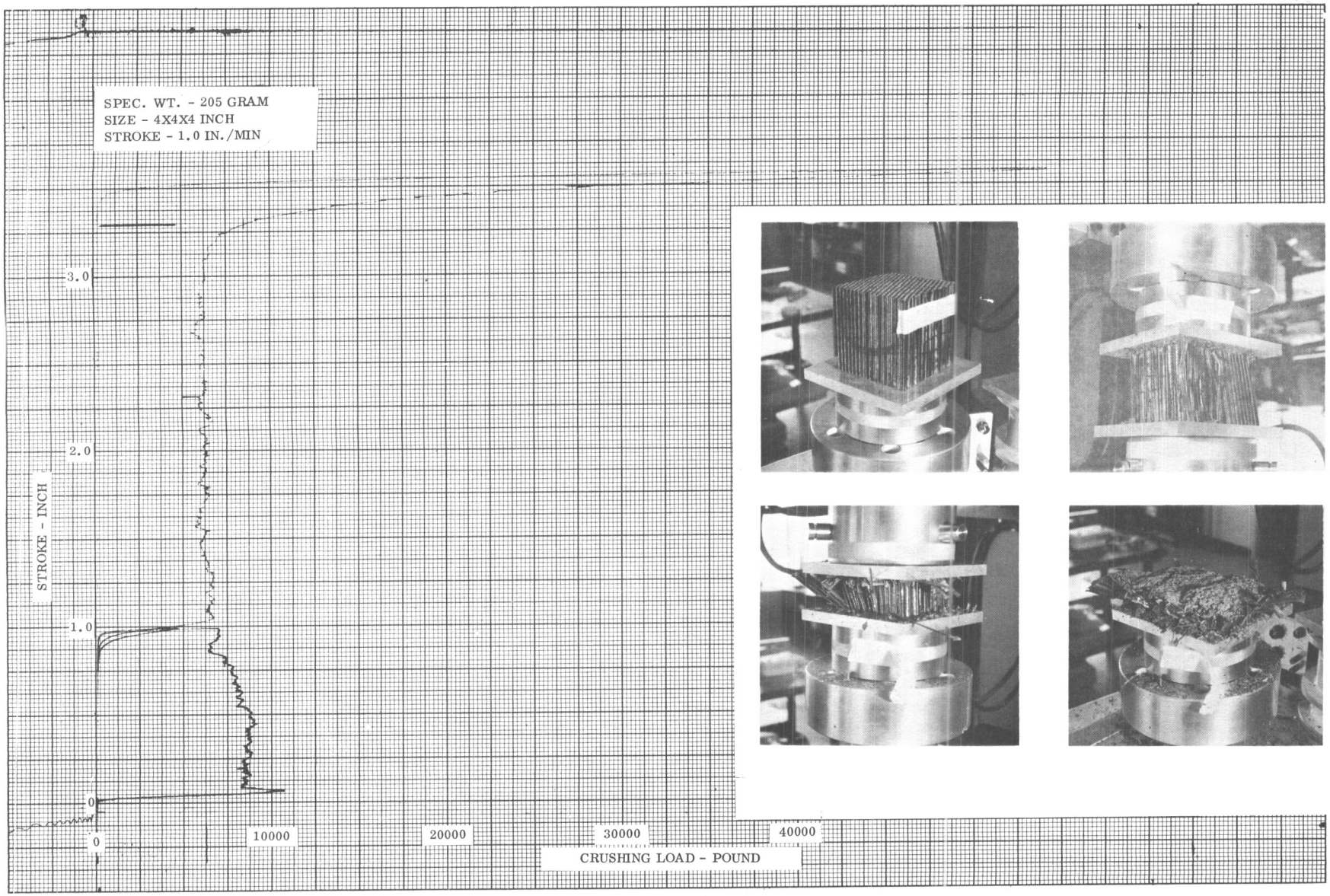

Test A-1i-d - Dovetail - 14 pcf

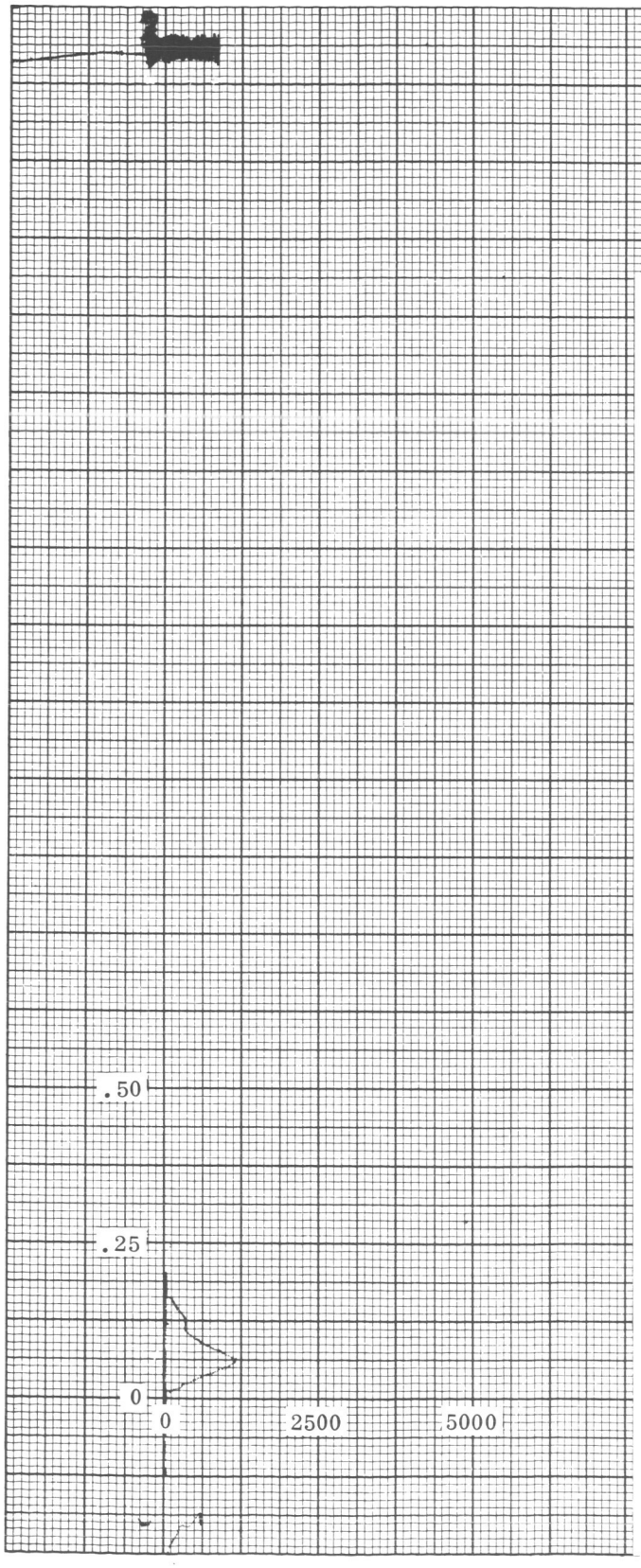

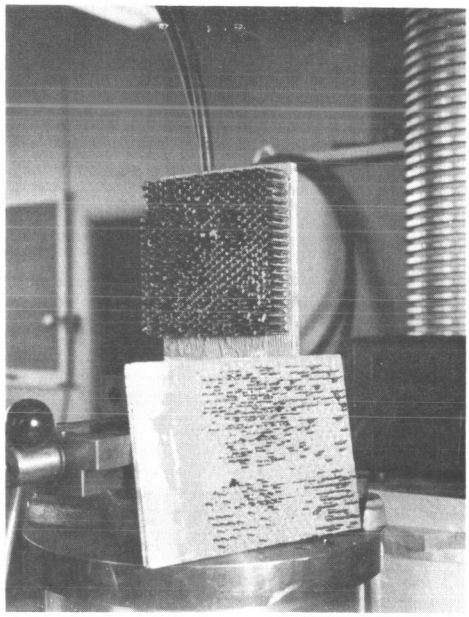

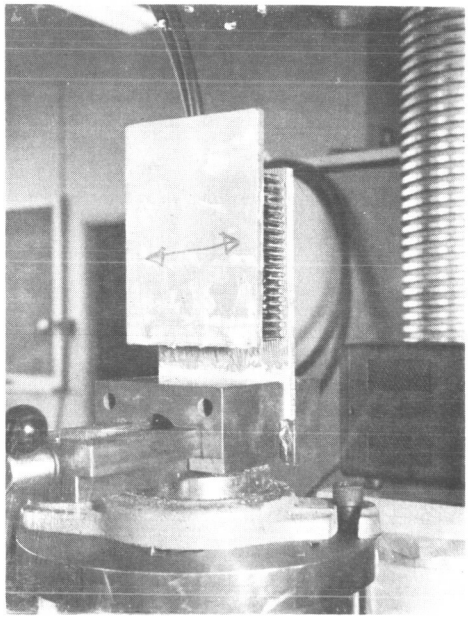

Test B-3-n Shear Test

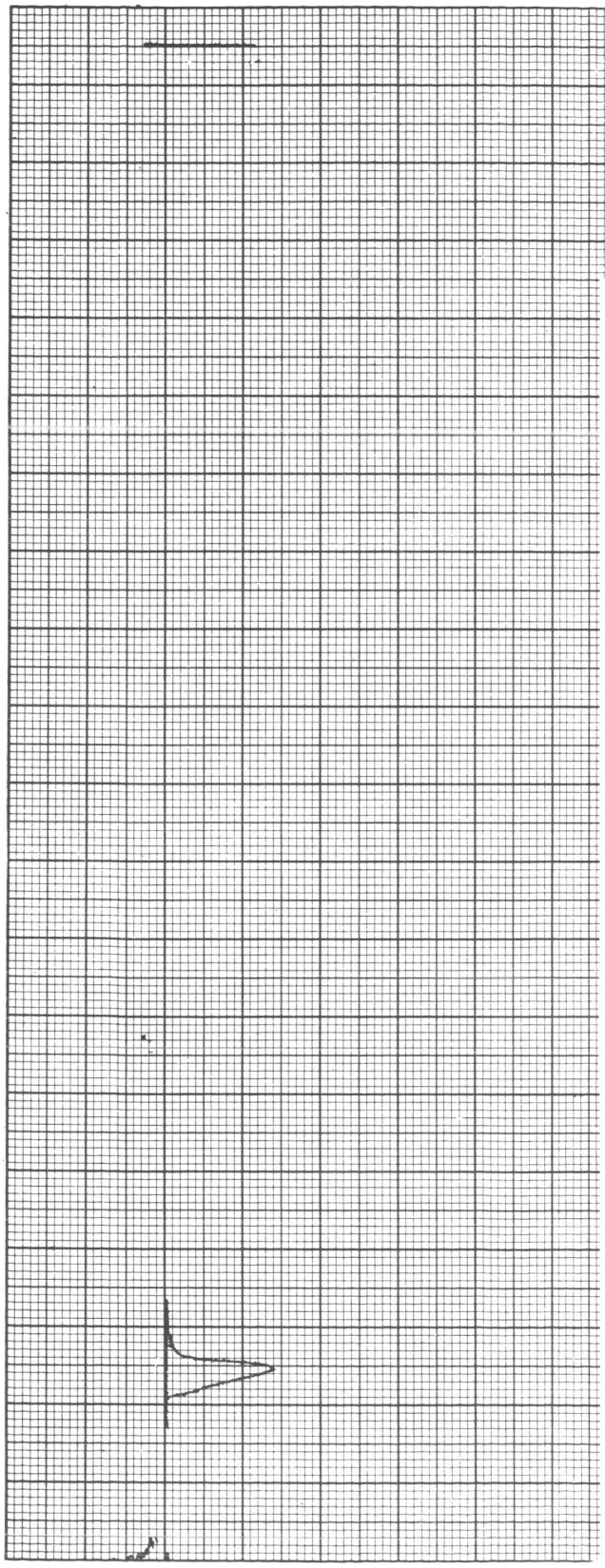

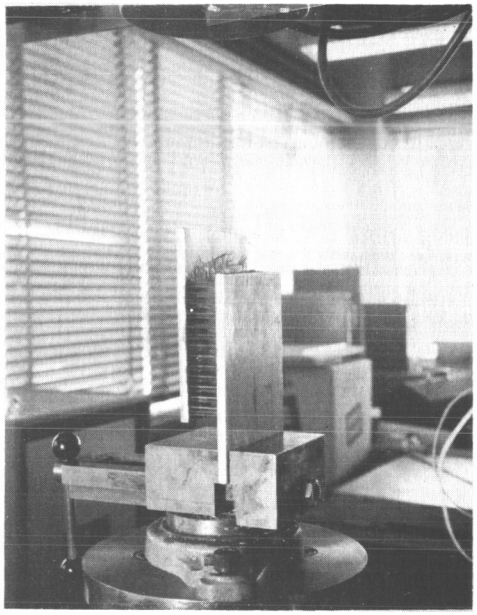

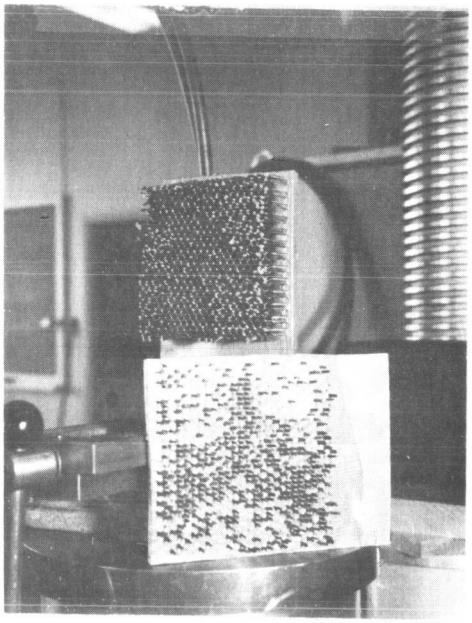

Test B-3-n Shear Test

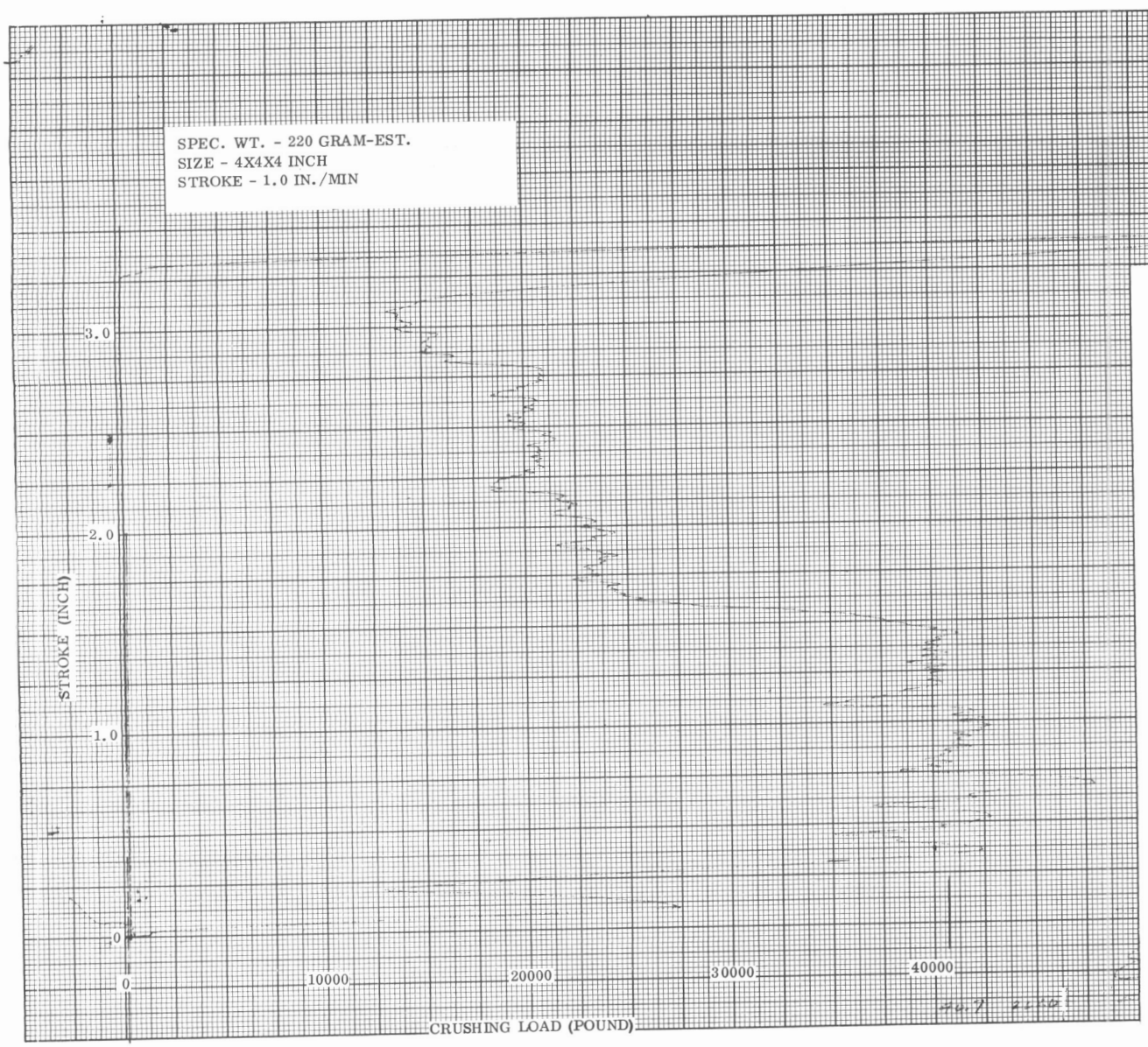

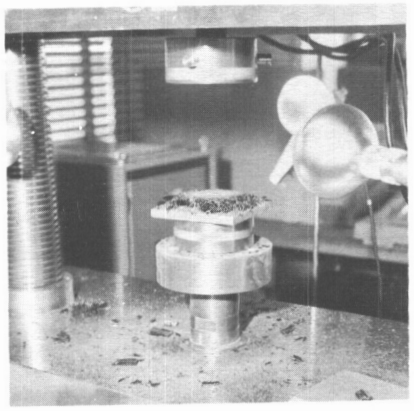

Test C-1-d - Temperature Equal 205^{o}F - 14 pcf

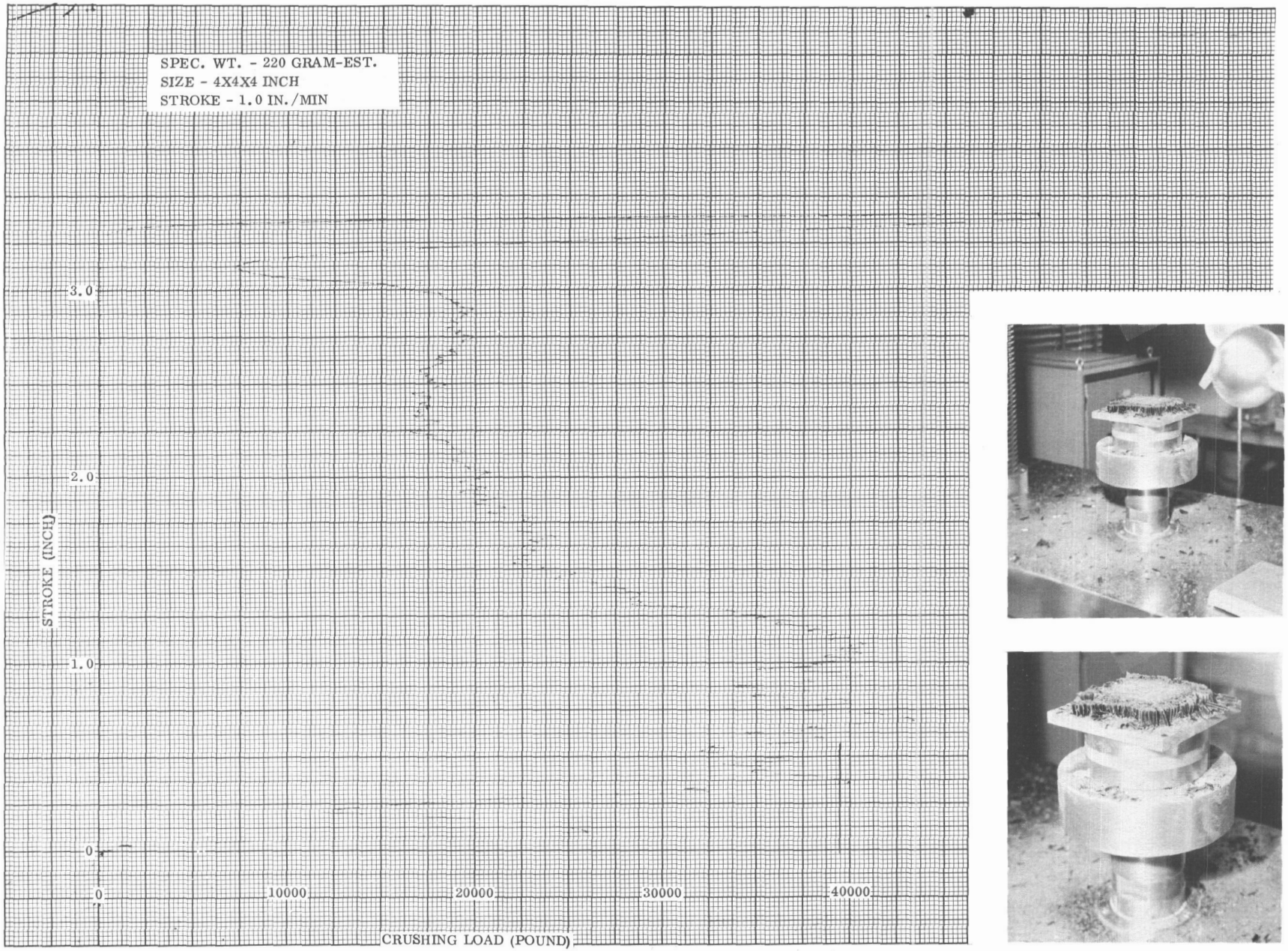

Test C-1-e - Temperature Equal 205^{o}F - 14 pcf

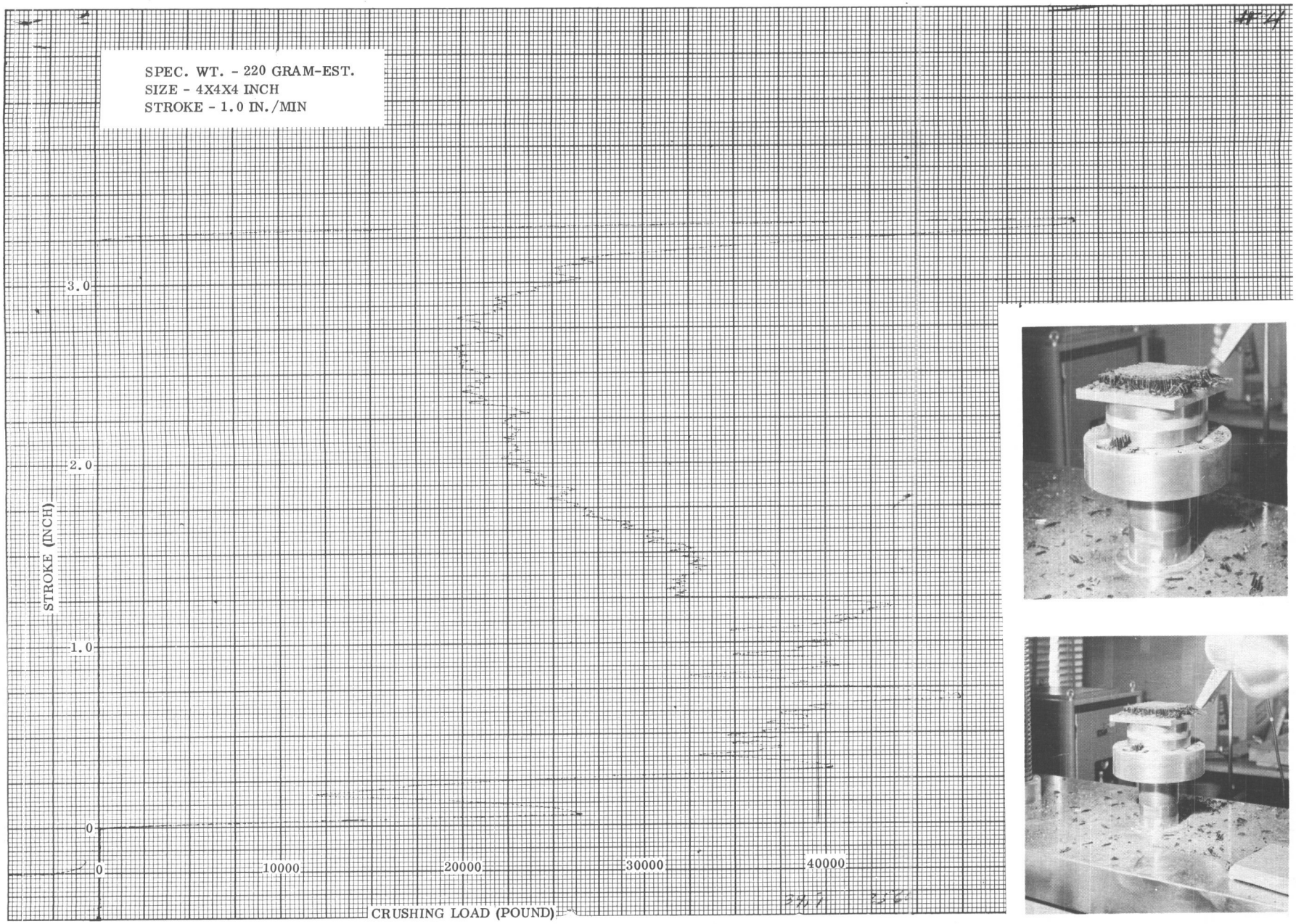

Test C-1-f - Temperature Equal 205°F - 14 pcf

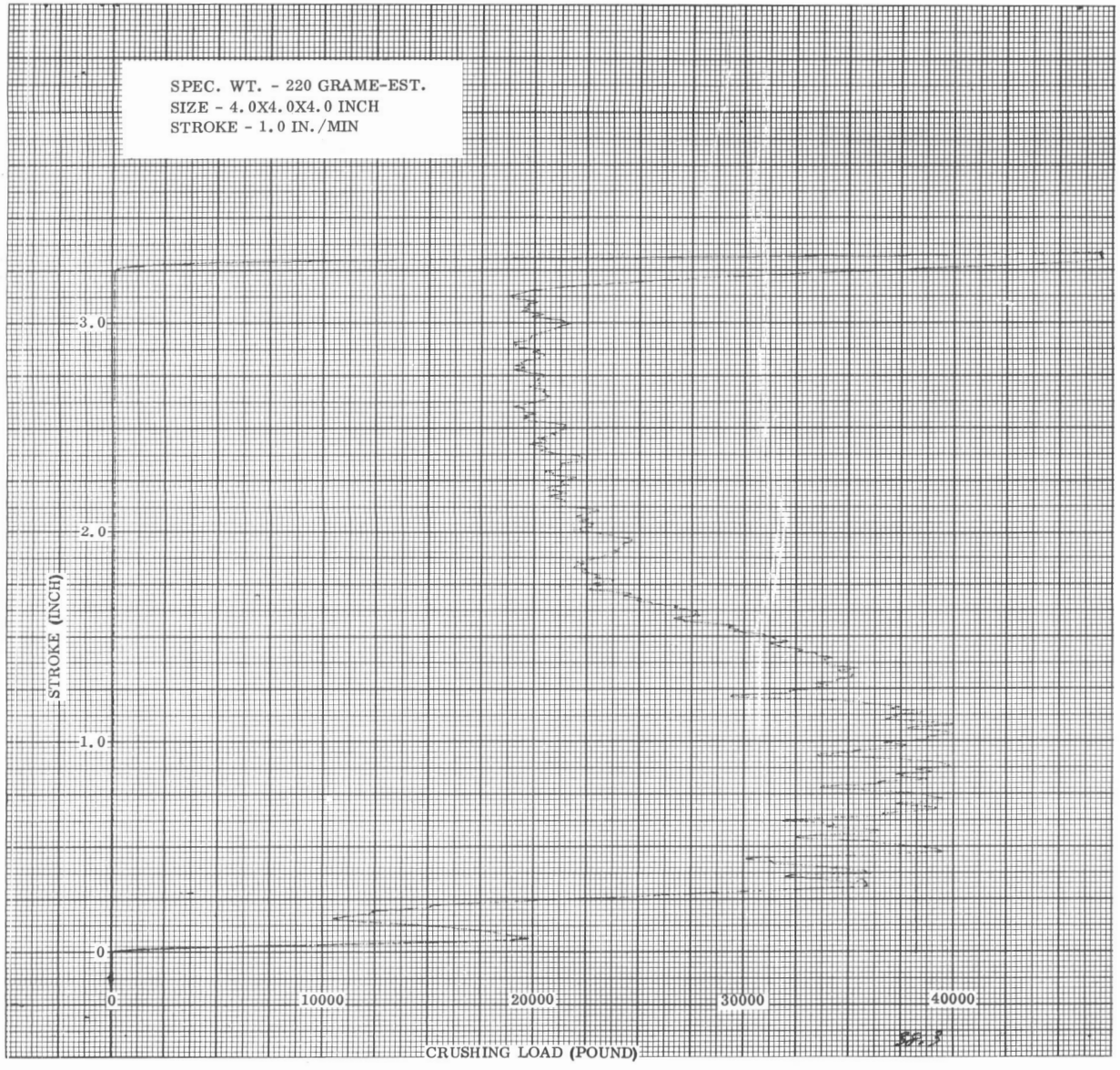

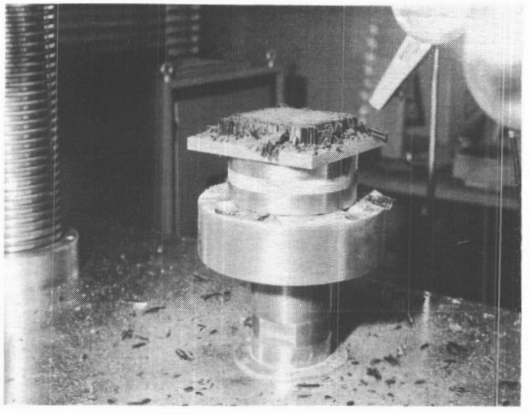

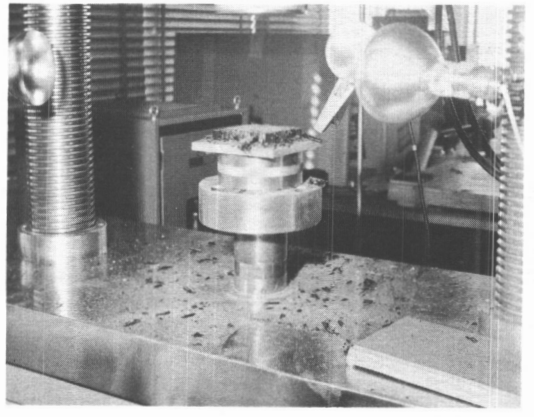

Test C-1-g - Temperature Equal 205°F - 14 pcf

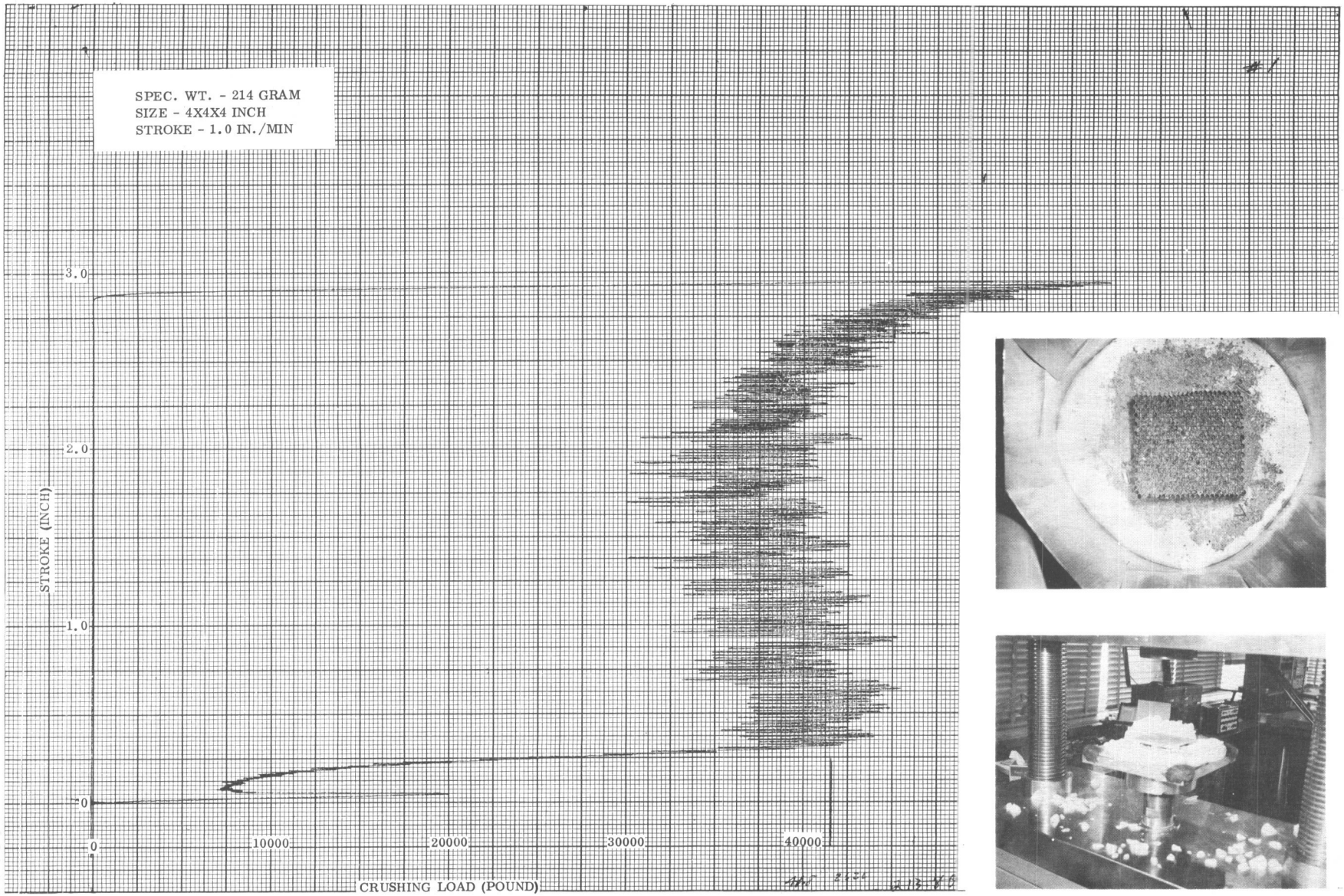

Test C-1-h - Temperature Equal 205°F - 14 pcf

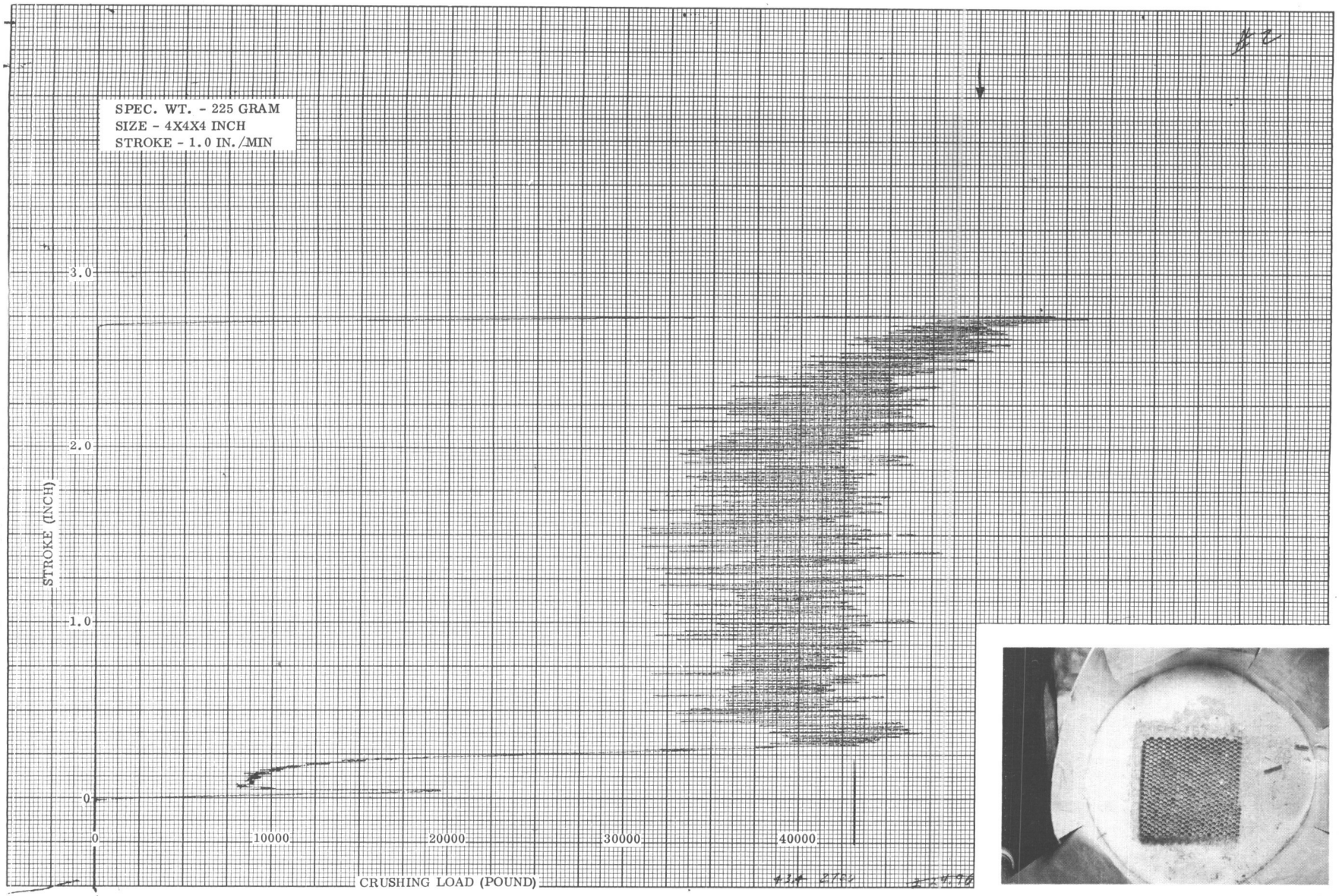

Test C-1-i - Temperature Equal -94^{O}F - 14 pcf

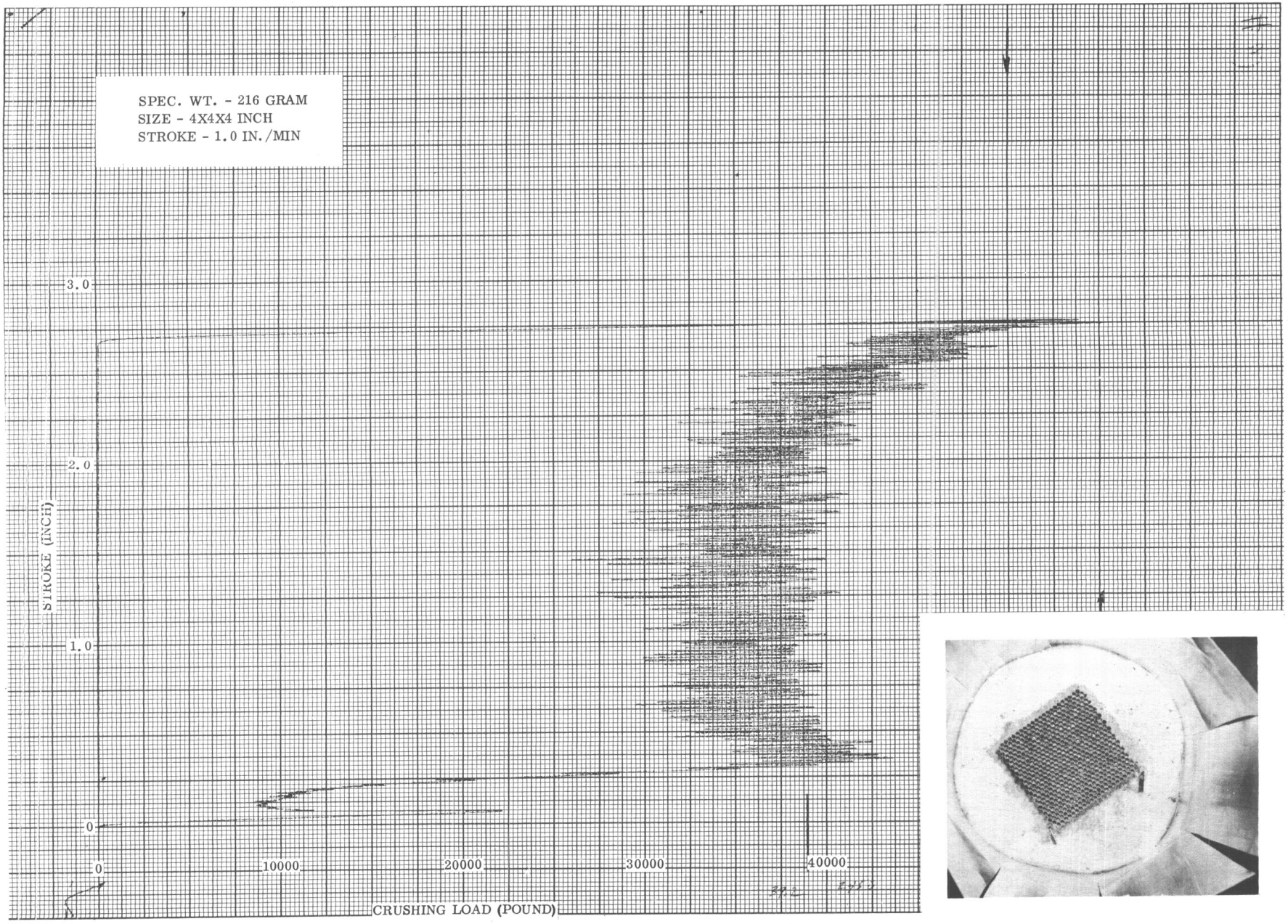

Test C-1-j - Temperature Equal -94°F - 14 pcf

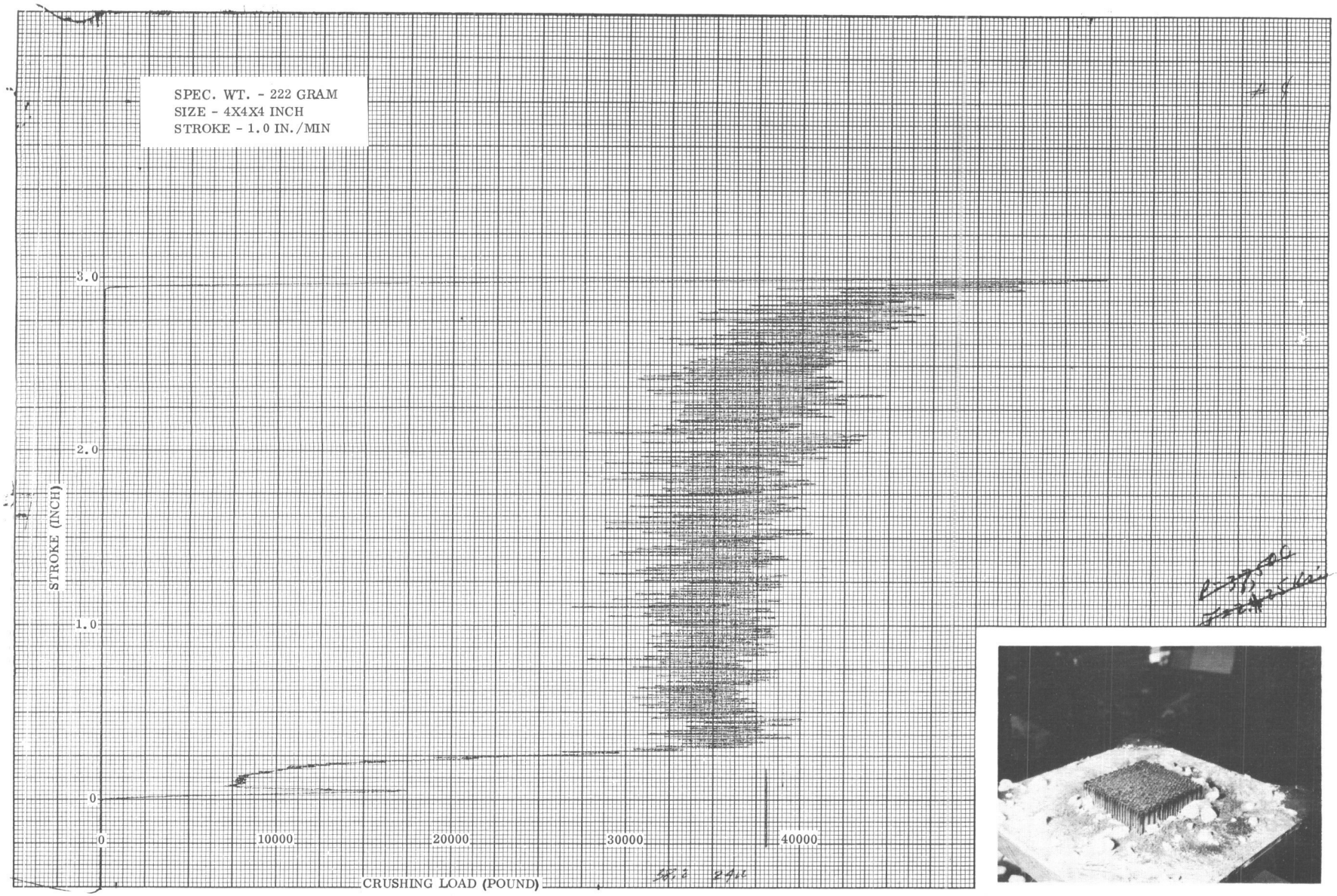

Test C-1-k - Temperature Equal -94°F - 14 pcf